Monthly Notices of the ROYAL ASTRONOMICAL SOCIETY
MNRAS **444,** 1318–1333 (2014) doi:10.1093/mnras/stu1516

The long-term rotation dynamics of neutron stars with differentially rotating unmagnetized core

D. P Barsukov,[1,2]★ O. A. Goglichidze[1]★ and A. I. Tsygan[1]★

[1]*Ioffe Physical-Technical Institute of the Russian Academy of Sciences, 194021 Saint-Petersburg, Russian Federation*
[2]*Saint-Petersburg State Polytechnical University, 195251 Saint-Petersburg, Russian Federation*

Accepted 2014 July 26. Received 2014 May 25; in original form 2014 January 15

ABSTRACT

We consider the pulsar long-term rotation dynamics taking into account the non-rigidity of neutron star rotation. We restrict our attention to the models with two essential assumptions: (1) crust–core interaction occurs via the viscosity (magnetic coupling is not important); (2) neutron star shape is symmetrical over the magnetic axis. The neutron star core is described by linearized quasi-stationary Newtonian hydrodynamical equations in one-fluid and two-fluid (neutron superfluidity) approximations. It is shown that in this case the pulsar inclination angle evolves to 0° or 90° very quickly. Since such fast evolution seems to contradict the observation data, either neutron stars are triaxial or the magnetic field plays the leading role in crust–core coupling.

Key words: dense matter – hydrodynamics – stars: neutron – pulsars: general.

1 INTRODUCTION

A rotating magnetized neutron star, if it has perfectly spherical shape, can be characterized by two vectors: angular velocity vector $\boldsymbol{\Omega}$ and magnetic moment vector $\boldsymbol{m}$. During the neutron star life the magnitudes of these vectors as well as the inclination angle χ between them evolve. The long-term rotation dynamics significantly depends on the model of the neutron star magnetosphere. According to the simplest vacuum model the angular momentum of neutron star is carried away only by magnetic dipole radiation. In this case, equation $\Omega \cos\chi = \text{const}$ should be satisfied. It makes all pulsars evolve to the co-axial state $\chi = 0$ (Beskin 2009).

The presence of plasma surrounding the neutron star affects the angular momentum loses in two ways. On the one hand, the plasma can effectively screen magnetic dipole radiation so that it can even absent at all (Beskin, Istomin & Philippov 2013). On the other hand, the longitudinal magnetospheric currents give rise to an additional angular momentum loses mechanism (Jones 1976; Beskin 2009). This current loses mechanism requires the satisfaction of equation $\Omega \sin\chi = \text{const}$. Thus, the inclination angle evolves with the same rate as in the case of vacuum model but in the opposite direction. The final state of all pulsars is the orthogonal rotation ($\chi = 90^\circ$).

If two these mechanisms operate simultaneously, the inclination angle evolves much more slowly (Barsukov, Goglichidze & Tsygan 2013a). Moreover, the presence of small-scale magnetic field at the surface of the neutron star can lead to the appearance of a stable equilibrium inclination angle between 0° and 90° (see Barsukov, Polyakova & Tsygan 2009 for the detail). The magnetohydrodynamic (MHD) simulations of pulsar magnetosphere also give the torque causing the quite slow angle evolution (Philippov, Tchekhovskoy & Li 2014).

The problem becomes even more complicated if one wants to take into account the internal structure of neutron star. Neutron star is not perfectly rigid. It contains a liquid core. The non-rigidity of star rotation results in that the anomalous electromagnetic torque directed perpendicular to the plane containing $\boldsymbol{\Omega}$ and $\boldsymbol{m}$ starts to affect the inclination angle evolution (Casini & Montemayor 1998; Barsukov et al. 2013a). The size of the effect is determined by particular crust–core interaction mechanism. Thus, long-term rotation dynamics becomes to be sensitive to the choice of the theory of neutron star interior as well as the magnetosphere theory.

There are two main mechanisms of crust–core interaction: magnetic coupling and viscosity (Easson 1979). The first mechanism is much more effective and if it takes place, protons, electrons and normal neutrons of neutron star core can be considered rigidly rotating with the crust. In contrast, the superfluid neutrons which are believed to be present in neutron star core (Yakovlev, Levenfish & Shibanov 1999) are decoupled from the rest of the matter and interact with it only by weak mutual friction force (vortex-mediated interaction) (Hall & Vinen 1956). It this case, the rate of the inclination angle evolution depends almost on the amount of the superfluid neutrons (Barsukov et al. 2013a; Barsukov, Goglichidze & Tsygan 2013b).

The configurations with magnetic field confined in neutron star crust are discussed in the literature too (Pons, Miralles & Geppert 2009; Gourgouliatos et al. 2013). The expulsion of magnetic field can be caused, for example, by first type superconductivity of core protons. Despite the fact that the second type proton superconductivity is more likely from the point of view of microscopic calculations (see, however Buckley, Metlitski & Zhitnitsky 2004),

★E-mail: bars@astro.ioffe.ru (DPB); goglichidze@gmail.com (OAG); tsygan@astro.ioffe.ru (AIT)

the situation in the neutron star rotation dynamics is not so clear. The coexistence of proton magnetic fluxoids with neutron superfluidity are inconsistent with observed long periods of neutron star precession (Link 2006).

In this paper, we investigate the long-term rotation dynamics of neutron star whose magnetic field does not penetrate the core. This research can be interesting by itself as a test for such magnetic field configurations. However, it also can be considered as a step to the more general model including core magnetic field.

The paper is organized as follows. In Section 2, we formulate the model and discuss the assumptions we make. Sections 3 and 4 are devoted to the effects of composition gradient and neutron superfluidity on the neutron star rotational dynamics respectively. In Section 5, we discuss the electromagnetic torque acting on the isolated neutron star. In Section 6, we present the pulsar inclination angle trajectories calculated for different neutron star parameters. Section 7 is devoted to discussion of the results.

2 MODEL

2.1 Basic assumptions

We will treat a neutron star as a spherical rigid shell containing a liquid core in a spherical cavity. The inner radius of the crust we will denote by r_c, the outer by r_{ns}. The crust rotates with angular velocity $\boldsymbol{\Omega}$. It feels the action of an external (electromagnetic) torque $\boldsymbol{K}$ which is supposed to be slowly varying in the reference frame corotating with the crust. The core acts on the crust with torque $\boldsymbol{N}$. Thus, the motion of the crust can be described by equation

$$I_{\rm crust}\dot{\boldsymbol{\Omega}} = \boldsymbol{K} + \boldsymbol{N}, \tag{1}$$

where $I_{\rm crust}$ is the crust moment of inertia and here and after we will use the notation $\dot{\boldsymbol{\Omega}} = d_t\boldsymbol{\Omega}$.

The neutron star core is described by system of hydrodynamical equations

$$\partial_t \boldsymbol{v} + (\boldsymbol{v}\cdot\nabla)\boldsymbol{v} + \nabla P/\rho + \nabla\Phi = \boldsymbol{f}_v, \tag{2}$$

$$\partial_t \rho + \mathrm{div}(\rho\boldsymbol{v}) = 0, \tag{3}$$

$$\Phi(\boldsymbol{r}) = -G\int \frac{\rho(\boldsymbol{r}')}{|\boldsymbol{r}-\boldsymbol{r}'|}\,\mathrm{d}^3 r', \tag{4}$$

where by the $\boldsymbol{f}_v$ we have denoted the viscous force acting on the unit mass if the liquid.

Through the paper, we will suppose for simplicity that the core liquid consists only of neutrons, protons and electrons (npe-matter). The neutron star core is isothermal with very good accuracy (Gnedin, Yakovlev & Potekhin 2001). Moreover, the matter constituting the core is strong degenerate. These facts allow us to represent the pressure gradient as

$$\nabla P = \rho_n\nabla\mu_n + \rho_p\nabla\mu_p + \rho_e\nabla\mu_e, \tag{5}$$

where μ_n, μ_p and μ_e are the neutron, proton and electron chemical potentials per unit mass, respectively, $\rho = \rho_n + \rho_p + \rho_e$.

Using the quasi-neutrality condition $\rho_p = (m_p/m_e)\rho_e$, one can rewrite equation (5) in the following form

$$\nabla P = \rho\nabla\mu_n + y\rho\nabla(\mu_c - \mu_n), \tag{6}$$

where we have formally introduced the effective chemical potential of the charged component of core matter

$$\mu_c = \frac{m_p\mu_p + m_e\mu_e}{m_p + m_e}. \tag{7}$$

Also we have denoted by y the relation ρ_c/ρ where $\rho_c = \rho_p + \rho_e$ is the charged component mass density.

Let us first consider the simplest case of constant y. The most convenient frame of reference for the analysis is the one corotating with the crust. In this frame equations (2) and (3) take the form

$$\partial_t^*\boldsymbol{u} + 2[\boldsymbol{\Omega}\times\boldsymbol{u}] + (\boldsymbol{u}\cdot\nabla)\boldsymbol{u} + \nabla\varkappa = -[\dot{\boldsymbol{\Omega}}\times\boldsymbol{r}] + \boldsymbol{f}_v, \tag{8}$$

$$\partial_t^*\rho + \mathrm{div}(\rho\boldsymbol{u}) = 0, \tag{9}$$

where we have introduced vector $\boldsymbol{u} = \boldsymbol{v} - [\boldsymbol{\Omega}\times\boldsymbol{r}]$ and function $\varkappa = \mu_n + y(\mu_c - \mu_n) + \Phi - \frac{1}{2}[\boldsymbol{\Omega}\times\boldsymbol{r}]^2$. Symbol ∂_t^* denotes the time derivative in the corotating frame of reference. Note that $d_t^*\boldsymbol{\Omega} = d_t\boldsymbol{\Omega} = \dot{\boldsymbol{\Omega}}$. From the point of view of an observer in the corotating frame, the non-uniformity of star rotation looks like the force spinning up the flow ($[\dot{\boldsymbol{\Omega}}\times\boldsymbol{r}]$ term in the right-hand side of equation 8).

Let us suppose that $\boldsymbol{u}$ is produced only by $\dot{\boldsymbol{\Omega}}$. If $\dot{\boldsymbol{\Omega}} = 0$, equation (8) reduces just to hydrostatical equilibrium equation

$$\nabla\left(\mu_n^{(0)} + y\left(\mu_c^{(0)} - \mu_n^{(0)}\right) + \Phi^{(0)} - \frac{1}{2}[\Omega\times\boldsymbol{r}]^2\right) = 0. \tag{10}$$

Here and after, index '(0)' denotes the hydrostatical values of variables. Through the paper, we will suppose that all hydrostatical variables are the functions only of the distance r from the star centre. Strictly speaking, it is not a self-consistent assumption because the centrifugal force (the last term in equation 10) breaks the spherical symmetry. However, it seems to be not very plausible that the inclusion of the centrifugal force can qualitatively change the results, at least for the slowly rotating neutron stars for which (as it will be seen below) the effects of non-rigidity of the core are most significant.

It will be useful to turn for a while to the dimensionless quantities: $\boldsymbol{r} = r_c\boldsymbol{x}$, $\nabla = r_c^{-1}\tilde{\nabla}$, $t = \tau/\Omega$, $\boldsymbol{\Omega} = \Omega\boldsymbol{e}_z$, $\dot{\boldsymbol{\Omega}} = \dot{\Omega}\boldsymbol{e}_{\dot{\Omega}}$, $\boldsymbol{u} = (\dot{\Omega}/\Omega)r_c\boldsymbol{q}$, $\varkappa = \Omega^2 r_c^2\tilde{\varkappa}$, $\rho = \rho^{(b)}\tilde{\rho}$, $\boldsymbol{f}_v = \dot{\Omega}r_c\tilde{\boldsymbol{f}}_v$. Here, $\rho^{(b)}$ is the hydrostatical value of the mass density of core liquid at the crust–core interface. The equations take the form:

$$\partial_\tau^*\boldsymbol{q} + 2[\boldsymbol{e}_z\times\boldsymbol{q}] + \epsilon(\boldsymbol{q}\cdot\tilde{\nabla})\boldsymbol{q} + \frac{1}{\epsilon}\tilde{\nabla}\tilde{\varkappa} = -[\boldsymbol{e}_{\dot{\Omega}}\times\boldsymbol{r}] + \tilde{\boldsymbol{f}}_v, \tag{11}$$

$$\partial_\tau^*\tilde{\rho} + \tilde{\nabla}\cdot(\tilde{\rho}\boldsymbol{q}) = 0, \tag{12}$$

where we have introduced a parameter $\epsilon = \dot{\Omega}/\Omega^2$. Note that here we have ignored the small dependence of Ω and $\dot{\Omega}$ on time. The validity of this assumption will be argued below.

Parameter ϵ is very small for neutron stars. It means that $\boldsymbol{u}$ is the small perturbation to the rigid rotation $[\boldsymbol{\Omega}\times\boldsymbol{r}]$. All variables can be expanded in powers of ϵ:

$$\tilde{\rho} = \tilde{\rho}^{(0)} + \epsilon\tilde{\rho}^{(1)} + O(\epsilon^2), \tag{13}$$

$$\tilde{\Phi} = \tilde{\Phi}^{(0)} + \epsilon\tilde{\Phi}^{(1)} + O(\epsilon^2), \tag{14}$$

$$\tilde{\mu}_\alpha = \tilde{\mu}_\alpha^{(0)} + \epsilon\tilde{\mu}_\alpha^{(1)} + O(\epsilon^2). \tag{15}$$

Substituting these expansions into equations (11) and (12), using equation (10) and neglecting the terms containing ϵ, one can obtain

$$\partial_\tau^*\boldsymbol{q} + 2\boldsymbol{e}_z\times\boldsymbol{q} + \tilde{\nabla}\tilde{\varkappa}^{(1)} = -[\boldsymbol{e}_{\dot{\Omega}}\times\boldsymbol{x}] + \tilde{\boldsymbol{f}}_v^{(1)}, \tag{16}$$

$$\partial^*_\tau \tilde{\rho}^{(1)} + \tilde{\nabla} \cdot \left(\tilde{\rho}^{(0)} \boldsymbol{q}\right) = 0. \tag{17}$$

Since we are interested in the velocities much smaller than the speed of sound the time-derivative term in equation (17) can be neglected:

$$\tilde{\nabla} \cdot \left(\tilde{\rho}^{(0)} \boldsymbol{q}\right) = 0. \tag{18}$$

It is important to note that the smallness of temperature term in equation (5) allows us to exclude from the consideration the equation (4) relating $\rho^{(1)}$ with $\Phi^{(1)}$ (if one does not want to calculate $\rho^{(1)}$, $\mu^{(1)}$ or $\Phi^{(1)}$). As a result, velocity perturbation equation (16) formally coincides with corresponding equation for incompressible fluid without gravitational force acting on it. However, the compressibility modifies the continuity equation.

After returning to dimensional variables, equations take the form

$$\partial^*_{\rm t} \boldsymbol{u} + 2\boldsymbol{\Omega} \times \boldsymbol{u} + \nabla \varkappa^{(1)} = -[\dot{\boldsymbol{\Omega}} \times \boldsymbol{r}] + \boldsymbol{f}^{(1)}_{\rm v}, \tag{19}$$

$$\mathrm{div}\left(\rho^{(0)} \boldsymbol{u}\right) = 0. \tag{20}$$

These equations together with equation (1) and boundary condition

$$\boldsymbol{u}_{r=r_{\rm c}} = 0 \tag{21}$$

describe star rotational dynamics. In the absence of magnetic field, only viscosity can transfer angular momentum from the core into the crust. The time-scale $t_{\rm v}$ of this transferring is much less than the typical time interval t_x during which the vectors $\boldsymbol{\Omega}$ and $\dot{\boldsymbol{\Omega}}$ change significantly. As long as $t \ll t_x$, these vectors can be considered constant. On the other hand, after $t \gg t_{\rm v}$ the solution of equations (19) and (20) with constant $\boldsymbol{\Omega}$ and $\dot{\boldsymbol{\Omega}}$ relaxes to stationary flow and time derivative term $\partial^*_{\rm t} \boldsymbol{u}$ in equation (19) becomes negligibly small. Since $t_x \gg t_{\rm v}$, despite the slow changing of vectors $\boldsymbol{\Omega}$ and $\dot{\boldsymbol{\Omega}}$, the flow remains quasi-stationary. Thus, equation (19) can be replaced by the stationary equation

$$2\boldsymbol{\Omega} \times \boldsymbol{u} + \nabla \varkappa^{(1)} = -[\dot{\boldsymbol{\Omega}} \times \boldsymbol{r}] + \boldsymbol{f}^{(1)}_{\rm v}. \tag{22}$$

After $t \gg t_{\rm v}$, the flow 'forgets' the initial condition and at each time point it is determined only by instant values of $\boldsymbol{\Omega}$ and $\dot{\boldsymbol{\Omega}}$ depending on time only through these two vectors.

The viscosity force can be represented in the form (Landau et al. 1959)

$$f^i_{\rm v} = \frac{1}{\rho} \frac{\partial}{\partial r^k} \pi^{ik}, \tag{23}$$

where

$$\pi^{ik} = \eta \left(\frac{\partial v^i}{\partial r^k} + \frac{\partial v^k}{\partial r^i} - \frac{2}{3} \delta^{ik} \mathrm{div} \boldsymbol{v} \right) + \zeta \delta^{ik} \mathrm{div} \boldsymbol{v} \tag{24}$$

is the viscous stress tensor, η and ζ are the coefficients of shear and bulk viscosities, respectively. Upper Latin indices denote the vector component in some arbitrary Cartesian basis, summation over repeated indices is implied.

Turning to the dimensionless variables and neglecting terms $\sim\epsilon$, one obtains

$$\pi^{ij(1)} \approx E\tilde{\eta}^{(0)} \left(\frac{\partial q^i}{\partial x^k} + \frac{\partial q^k}{\partial x^i} - \frac{2}{3} \delta^{ik} \tilde{\nabla} \cdot \boldsymbol{q} \right) + E' \tilde{\zeta}^{(0)} \delta^{ik} \tilde{\nabla} \cdot \boldsymbol{q}, \tag{25}$$

$$\tilde{f}^{i(1)}_{\rm v} = \frac{1}{\tilde{\rho}^{(0)}} \left\{ E \frac{\partial}{\partial x^k} \left[\tilde{\eta}^{(0)} \left(\frac{\partial q^i}{\partial x^k} + \frac{\partial q^k}{\partial x^i} \right) \right] - \frac{\partial}{\partial x^i} \left[\left(\frac{2E}{3} \tilde{\eta}^{(0)} - E' \tilde{\zeta}^{(0)} \right) \tilde{\nabla} \cdot \boldsymbol{q} \right] \right\} \tag{26}$$

$$= \frac{1}{\tilde{\rho}^{(0)}} \left\{ E \left[\tilde{\eta}^{(0)} \tilde{\nabla}^2 q^i \right] + E \left(\frac{\partial q^i}{\partial x^k} + \frac{\partial q^k}{\partial x^i} \right) \frac{\partial \tilde{\eta}^{(0)}}{\partial x^k} + \left(\frac{2E}{3} \frac{\partial \tilde{\eta}^{(0)}}{\partial x^i} - E' \frac{\partial \tilde{\zeta}^{(0)}}{\partial x^i} \right) (\boldsymbol{q} \cdot \tilde{\nabla}) \ln \tilde{\rho}^{(0)} - \left(\frac{E}{3} \tilde{\eta}^{(0)} + E' \tilde{\zeta}^{(0)} \right) \frac{\partial}{\partial x^i} \left[(\boldsymbol{q} \cdot \tilde{\nabla}) \ln \tilde{\rho}^{(0)} \right] \right\}, \tag{27}$$

where $\eta = \eta^{(b)} \tilde{\eta}$, $\zeta = \zeta^{(b)} \tilde{\zeta}$, $\nu^{(b)}$ and $\zeta^{(b)}$ are the values of viscosity coefficients at the crust–core interface. We also have introduced two Ekman numbers

$$E = \frac{\eta^{(b)}}{\rho^{(b)} \Omega r_{\rm c}^2}, \quad E' = \frac{\zeta^{(b)}}{\rho^{(b)} \Omega r_{\rm c}^2}. \tag{28}$$

The last term in viscous force expression (27) was obtained with using equation (18). Two things should be pointed here. First, the Ekman numbers for the neutron star cores are very small (the numerical values will be discussed in Section 6). Secondly, the second derivatives of $\boldsymbol{q}$ are contained only in the first term of expression (27).

Angular momentum can diffuse from the centre of the core into the crust by the viscous tensions as soon as the differential rotation develops. The diffusion occurs on a characteristic time-scale of the order of $t_{\rm v} \sim (E\Omega)^{-1}$. However, in the case of small Ekman numbers, the more effective angular momentum transferring mechanism may take place, the so-called Ekman pumping. Let us now consider the ideas underlying the Ekman pumping in the framework of the simple case of $y = \mathrm{const}$. The possibilities of this mechanism in more realistic models and its contribution to the neutron star rotational dynamics will be discussed below.

2.2 Ekman pumping

Since E and $E' \ll 1$, it is reasonable to assume that $\boldsymbol{f}^{(1)}_{\rm v}$ much less than the other terms in equation (22). It plays the significant role only in the thin boundary layer where the flow should adjust to the viscous boundary condition (21) and spatial derivatives become large. The common approach to this problem is the following (Greenspan, 1990). Near the boundary, the velocity field $\boldsymbol{q}$ and function $\varkappa$ are split in two parts:

$$\boldsymbol{q} = \boldsymbol{q}_{\rm (in)} + \boldsymbol{q}_{(l)}, \ \varkappa^{(1)} = \varkappa_{\rm (in)} + \varkappa_{(l)}, \tag{29}$$

where $(\boldsymbol{q}_{\rm (in)}, \varkappa_{\rm (in)})$ is the solution of the ideal hydrodynamics equations and $(\boldsymbol{q}_{(l)}, \varkappa_{(l)})$ is the correction to the $(\boldsymbol{q}_{\rm (in)}, \varkappa_{\rm (in)})$ due to viscosity. This correction should rapidly disappear depthward the core.

For $\boldsymbol{q}_{\rm (in)}$, we have

$$2[\boldsymbol{e}_z \times \boldsymbol{q}_{\rm (in)}] + \tilde{\nabla} \tilde{\varkappa}_{\rm (in)} = -[\boldsymbol{e}_{\dot{\Omega}} \times \boldsymbol{x}], \tag{30}$$

$$\tilde{\nabla} \cdot \left(\tilde{\rho}^{(0)} \boldsymbol{q}_{\rm (in)}\right) = 0, \tag{31}$$

$$\left(\boldsymbol{q}_{\rm (in)} \cdot \boldsymbol{e}_r\right)_{r=r_{\rm c}} = 0, \tag{32}$$

where $\boldsymbol{e}_r = \boldsymbol{r}/r$ is the unit normal vector to the internal crust surface. Here, we are compelled to replace boundary condition (21) by the impermeability condition restricting only the normal component of $\boldsymbol{q}$.

The basic assumption about (l)-functions is that instead of the usual radial coordinate x they depend on the stretched one

$\xi = E^{-1/2}(1-x)$, so,

$$(\boldsymbol{e}_r\cdot\tilde{\nabla})\left(\boldsymbol{q}_{(l)},\ \tilde{\varkappa}_{(l)}\right) = -E^{-1/2}\partial_\xi\left(\boldsymbol{q}_{(l)},\ \tilde{\varkappa}_{(l)}\right) \sim O(E^{-1/2}). \quad (33)$$

Note, however, that the tangent derivative of any function is still

$$\tilde{\nabla}_\perp\left(\boldsymbol{q}_{(l)},\ \tilde{\varkappa}_{(l)}\right) \sim O(1). \quad (34)$$

Substituting equations (30) and (27) into (22), using (34), (33) and (29) and neglecting all terms containing positive powers of E and E', one can obtain

$$2[\boldsymbol{e}_z\times\boldsymbol{q}_{(l)}] - \boldsymbol{e}_r E^{-1/2}\partial_\xi\tilde{\varkappa}_{(l)} = \partial_\xi^2\boldsymbol{q}_{(l)}. \quad (35)$$

The right-hand side of the equation arises from the first term from viscous force expression (27) (the only term containing second derivative with respect to ξ).

Continuity equation can be expressed as

$$\tilde{\rho}^{(0)}(\boldsymbol{e}_r\cdot\tilde{\nabla})(\boldsymbol{e}_r\cdot\boldsymbol{q}_{(l)}) + (\boldsymbol{e}_r\cdot\boldsymbol{q}_{(l)})\tilde{\nabla}\cdot\left(\tilde{\rho}^{(0)}\boldsymbol{e}_r\right) + \tilde{\rho}^{(0)}\boldsymbol{e}_r\cdot\tilde{\nabla}\times[\boldsymbol{e}_r\times\boldsymbol{q}_{(l)}] = 0. \quad (36)$$

The first term here larger than the second by the factor $E^{-1/2}$ (see equality 33) and, thus, the second term can be neglected. It gives the simple equation relating normal $\boldsymbol{q}_{r(l)}$ and tangent $\boldsymbol{q}_{tg(l)}$ components of $\boldsymbol{q}_{(l)}$:

$$E^{-1/2}\partial_\xi q_{r(l)} = \boldsymbol{e}_r\cdot\tilde{\nabla}\times[\boldsymbol{e}_r\times\boldsymbol{q}_{tg(l)}]. \quad (37)$$

The full velocity field should be equal to zero at the crust–core interface:

$$\left(\boldsymbol{q}_{(\mathrm{in})} + \boldsymbol{q}_{(l)}\right)_{r=r_\mathrm{c}} = 0. \quad (38)$$

According to boundary conditions (32) and (38) $q_{r(l)} = 0$ at the crust–core interface. Hence, using equation (37) one can estimate $q_{r(l)} \sim E^{1/2}q_{tg(l)}$. The boundary layer correction is almost tangent, thus, instead of equation (35) one can consider equation

$$2[\boldsymbol{e}_z\times\boldsymbol{q}_{tg(l)}] - \boldsymbol{e}_r E^{-1/2}\partial_\xi h_{(l)} = \partial_\xi^2\boldsymbol{q}_{tg(l)}. \quad (39)$$

Integration of this equation with boundary condition (38) gives

$$(i\boldsymbol{q}_{tg(l)} + \boldsymbol{e}_r\times\boldsymbol{q}_{tg(l)}) = -(i\boldsymbol{q}_{tg(\mathrm{in})} + \boldsymbol{e}_r\times\boldsymbol{q}_{tg(\mathrm{in})})_{r=r_\mathrm{c}}\exp\left[-(1\pm i)|\boldsymbol{e}_r\cdot\boldsymbol{e}_z|^{1/2}\xi\right]. \quad (40)$$

Here, symbol '$\pm$' denotes the sign of scalar product $(\boldsymbol{e}_r\cdot\boldsymbol{e}_z)$. Substituting expression (40) into equation (37), integrating over ξ from 0 to ∞ and taking into account boundary condition (38), one can obtain

$$q_{r(\mathrm{in})}|_{r=r_\mathrm{c}} = -q_{r(l)}|_{r=r_\mathrm{c}} = -\frac{1}{2}E^{1/2}\boldsymbol{e}_r\cdot\tilde{\nabla}\times\left[\frac{\boldsymbol{e}_r\times\boldsymbol{q}_{tr(\mathrm{in})}\pm\boldsymbol{q}_{tr(\mathrm{in})}}{|\boldsymbol{e}_r\cdot\boldsymbol{e}_z|^{1/2}}\right]_{r=r_\mathrm{c}}. \quad (41)$$

As a result, the presence of the Ekman layer reduces just to the specific boundary condition (41). Turning back to dimensional variables, we have

$$2[\boldsymbol{\Omega}\times\boldsymbol{u}] + \nabla\varkappa^{(1)} = -[\dot{\boldsymbol{\Omega}}\times\boldsymbol{r}], \quad (42)$$

$$\mathrm{div}\left(\rho^{(0)}\boldsymbol{u}\right) = 0, \quad (43)$$

$$(\boldsymbol{e}_r\cdot\boldsymbol{u})_{r=r_\mathrm{c}} = -\frac{1}{2}r_\mathrm{c}E^{1/2}\boldsymbol{e}_r\cdot\mathrm{curl}\left[\frac{\boldsymbol{e}_r\times\boldsymbol{u}\pm\boldsymbol{u}}{|\boldsymbol{e}_r\cdot\boldsymbol{e}_z|^{1/2}}\right]_{r=r_\mathrm{c}}. \quad (44)$$

Note that now we have denoted by $\boldsymbol{u}$ and $h^{(1)}$ the bulk values of these quantities.

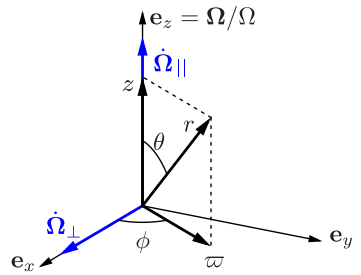

Figure 1. Vectors and coordinates used in Section 2.2.

Let us for clarity consider the axisymmetric star braking. From the physical point of view, the situation is the following. The crust is braked by external torque and, thus, it rotates slower than the core. Directly by the viscous force the crust can retard the rotation of the fluid only in the thin boundary layer. However, it leads to decreasing of the Coriolis force in that region and, thus, produces the flow towards the rotational axes along the boundary layer. To compensate for the layer mass current, small ($\sim E^{1/2}$) secondary flow in the bulk of the core should take place. The non-axisymmetric external torque produces the more complicated flow structure but qualitatively the physical processes are the same.

Equations (42)–(44) allow us to express $\boldsymbol{u}$ and $\varkappa$ as functions of $\boldsymbol{\Omega}$ and $\dot{\boldsymbol{\Omega}}$. In order to do this, it is useful to represent $\dot{\boldsymbol{\Omega}}$ as a sum of two vectors $\dot{\boldsymbol{\Omega}}_{||}$ and $\dot{\boldsymbol{\Omega}}_\perp$, where $\dot{\boldsymbol{\Omega}}_{||} = \boldsymbol{\Omega}(\boldsymbol{\Omega}\cdot\dot{\boldsymbol{\Omega}})/\Omega^2$ and $\dot{\boldsymbol{\Omega}}_\perp = \dot{\boldsymbol{\Omega}} - \dot{\boldsymbol{\Omega}}_{||}$. This expansion allows us to introduce the system of three orthonormal vectors $(\boldsymbol{e}_x,\ \boldsymbol{e}_y,\ \boldsymbol{e}_z)$, where $\boldsymbol{e}_z = \boldsymbol{\Omega}/\Omega$, $\boldsymbol{e}_x = \dot{\boldsymbol{\Omega}}_\perp/\dot{\Omega}_\perp$, $\boldsymbol{e}_y = [\boldsymbol{e}_z\times\boldsymbol{e}_x]$.

Furthermore, we will use the cylindrical (ϖ,ϕ,z) and spherical (r,θ,ϕ) coordinates defined as it is shown in Fig. 1.

The velocity field and potential $\varkappa^{(1)}$ as functions of $\boldsymbol{\Omega}$ and $\dot{\boldsymbol{\Omega}}$ have the following form:

$$\boldsymbol{u} = [\boldsymbol{w}\times\boldsymbol{r}] - \frac{\dot{\Omega}_{||}}{2\Omega}\left[\boldsymbol{e}_\varpi\varpi + \boldsymbol{e}_z\frac{1}{\rho^{(0)}}\int_0^z\frac{1}{\varpi}\frac{\partial}{\partial\varpi}\left(\varpi^2\rho^{(0)}\right)\mathrm{d}z'\right] - \boldsymbol{e}_z E^{1/2}\frac{\dot{\Omega}_\perp}{4\Omega}\frac{\rho^{(b)}}{\rho^{(0)}}\left(\frac{r_\mathrm{c}}{z_b}\right)^{3/2}\left(3\varpi\sin\phi + \frac{r_\mathrm{c}}{z_b}\varpi\cos\phi\right)\Bigg], \quad (45)$$

$$\varkappa^{(1)} = -\dot{\Omega}_\perp z\varpi\sin\phi - \dot{\Omega}_{||}\int_0^\varpi\psi(\varpi)\varpi\,\mathrm{d}\varpi, \quad (46)$$

where

$$\boldsymbol{w} = -\frac{\dot{\Omega}_{||}}{2\Omega}\psi(\varpi)\boldsymbol{e}_z + \boldsymbol{e}_z\times\frac{\dot{\boldsymbol{\Omega}}_\perp}{\Omega}, \quad (47)$$

$$\psi(\varpi) = \left(\frac{|\boldsymbol{e}_r\cdot\boldsymbol{e}_z|}{E}\right)^{1/2}\frac{2J_\rho}{\rho^{(b)}r_\mathrm{c}} - \frac{1}{\rho^{(b)}r_\mathrm{c}}\frac{1}{\varpi}\frac{\mathrm{d}}{\mathrm{d}\varpi}\left(\varpi^2 J_\rho - r_\mathrm{c}^2\rho^{(b)}z_b\right) \quad (48)$$

$$\approx \left(\frac{|\boldsymbol{e}_r\cdot\boldsymbol{e}_z|}{E}\right)^{1/2}\frac{2J_\rho}{\rho^{(b)}r_\mathrm{c}}, \quad (49)$$

$$J_\rho = \int_0^{z_b}\rho^{(0)}\,\mathrm{d}z,\quad z_b = \sqrt{r_\mathrm{c}^2 - \varpi^2}. \quad (50)$$

These expressions are given up to the terms $\sim E^{1/2}$.

The velocity field consists of two parts proportional to $\dot{\Omega}_{||}$ and $\dot{\Omega}_\perp$. The first is the core response to the star braking, the second

is caused by the moving of the rotational axis over the star. We will call for short these parts 'parallel' and 'perpendicular' flows, respectively. Each of these flows consists of a small additional to $\mathbf{\Omega}$ fluid rotation and the secondary flow due to Ekman pumping.

The 'parallel' flow is axisymmetric. The angular momentum is carried into the crust by the secondary poloidal flow. The existence of such a flow requires much larger ($\sim E^{-1/2}$) toroidal current for the boundary condition (44) to be satisfied. The core rotates differentially with angular velocity

$$\left(\Omega - \frac{\dot{\Omega}_{||}}{\Omega}\psi(\varpi)\right)\boldsymbol{e}_z, \tag{51}$$

but everywhere faster ($\dot{\Omega}_{||} < 0$) than the crust. The smaller the Ekman number E, the weaker the interaction and the greater the lag between crust and core rotations.

If the external torque is not axisymmetric, the orientation of angular velocity of the core should slightly depart from $\boldsymbol{e}_z$. It is described by the 'perpendicular' flow. In the quasi-stationary state the core rotates rigidly with angular velocity

$$\mathbf{\Omega} + \boldsymbol{e}_z \times \frac{\dot{\mathbf{\Omega}}_{\perp}}{\Omega}. \tag{52}$$

It is important to note that in contrast to 'parallel' flow, here the lag between crust and core rotation does not depend on E. It is easy to verify that

$$\boldsymbol{u} = \left[\boldsymbol{e}_z \times \frac{\dot{\mathbf{\Omega}}_{\perp}}{\Omega}\right] \times \boldsymbol{r}, \tag{53}$$

$$\varkappa^{(1)} = -\dot{\Omega}_{\perp} z\varpi \sin\phi \tag{54}$$

formally is the exact solution of equations (42) and (43) with $\dot{\mathbf{\Omega}} = \dot{\mathbf{\Omega}}_{\perp}$. However, it does not satisfy boundary condition (44). This solution does not have physical meaning because there is no relaxation mechanism supporting quasi-stationarity. The relaxation is provided by viscosity whose effect is reduced to the boundary condition (44) when $E \ll 1$. The Ekman layer produces the secondary flow $\sim E^{1/2}$ along $\boldsymbol{e}_z$ which does not change the core angular velocity value but forces its direction to follow the moving of $\mathbf{\Omega}$.

Let us point the difference between 'parallel' and 'perpendicular' flows. In the first case, the angular momentum flux caused by 'force' $[\dot{\mathbf{\Omega}}_{||} \times \boldsymbol{r}]$, whereas in the second case, it is produced by the boundary condition. This is why 'parallel' flow larger by the factor $E^{-1/2}$.

The obtained expressions are appropriate in almost the whole core except the small region near the equator ($\varpi \to r_c$) where the secondary 'perpendicular' flow formally diverges. In that region the Ekman layer approximation is not applicable. As it can be seen from expression (40), the thickness of the Ekman layer is of the order of $r_c(E/|\boldsymbol{e}_z \cdot \boldsymbol{e}_r|)^{1/2}$. It becomes to be not thin there. The boundary becomes almost vertical and more self-consistent consideration requires the effects of vertical boundary layers to be taken into account (Greenspan 1990). However, we will not use the expressions for the secondary flows calculating the angular momentum transfer into the crust, therefore this divergence does not affect the result.

2.3 Angular momentum transfer

According to the model the system of equations (1), (19), (20), (21) allows us to investigate the time evolution of $\mathbf{\Omega}$ under the action of external torque $\boldsymbol{K}$. In order to close this system of equations one needs to calculate the interaction torque $\boldsymbol{N}$. In the quasi-stationary regime this torque is determined by instant values of $\mathbf{\Omega}$ and $\dot{\mathbf{\Omega}}$. Since we have supposed that there is no sources of $\boldsymbol{u}$ except $\dot{\mathbf{\Omega}}$, the interaction torque can be represented in the following form:

$$\begin{aligned}\boldsymbol{N} = &-S_1 I_{\rm core}\boldsymbol{e}_z(\boldsymbol{e}_z \cdot \dot{\mathbf{\Omega}}) - S_2 I_{\rm core}\boldsymbol{e}_z \times [\boldsymbol{e}_z \times \dot{\mathbf{\Omega}}] \\ &+ S_3 I_{\rm core}[\boldsymbol{e}_z \times \dot{\mathbf{\Omega}}],\end{aligned} \tag{55}$$

where $I_{\rm core}$ is the core moment of inertia and S_1, S_2, S_3 are some dimensionless coefficients.

Coefficient S_1 can be easily obtained from the angular momentum conservation law. For the core angular momentum $\boldsymbol{M}_{\rm core}$, it has the form

$$d_t \boldsymbol{M}_{\rm core} = -\boldsymbol{N}. \tag{56}$$

As well as the local quantities, angular momentum $\boldsymbol{M}_{\rm core}$ can be expanded in the powers of ϵ: $\boldsymbol{M}_{\rm core} = I_{\rm core}\mathbf{\Omega} + \boldsymbol{M}^{(1)}_{\rm core} + O(\epsilon^2)$. Taking the time derivative and changing to the corotating frame of reference, one can obtain

$$\begin{aligned} d_t \boldsymbol{M}_{\rm core} &\approx I_{\rm core}\dot{\mathbf{\Omega}} + d_t \boldsymbol{M}^{(1)}_{\rm core} \\ &= I_{\rm core}\dot{\mathbf{\Omega}} + d^*_t \boldsymbol{M}^{(1)}_{\rm core} + \mathbf{\Omega} \times \boldsymbol{M}^{(1)}_{\rm core} \\ &\approx I_{\rm core}\dot{\mathbf{\Omega}} + \mathbf{\Omega} \times \boldsymbol{M}^{(1)}_{\rm core}. \end{aligned} \tag{57}$$

Here, term $d^*_t \boldsymbol{M}^{(1)}_{\rm core}$ was neglected according to the quasi-stationarity approximation. Substituting equations (56) and (57) into equation (1) and multiplying the result by $\boldsymbol{e}_z$ one can obtain

$$(I_{\rm crust} + I_{\rm core})\left(\boldsymbol{e}_z \cdot \dot{\mathbf{\Omega}}\right) = \boldsymbol{e}_z \cdot \boldsymbol{K}. \tag{58}$$

Substituting interaction torque expression (55) into equation (1) and again multiplying the result by $\boldsymbol{e}_z$, after comparing the obtained expression with equation (58) one can see that $S_1 = 1$. It is important to note that this result is not a feature of Ekman mechanism. It is a general property of the quasi-stationary flows.

Strong coupling regime corresponds to $S_2 \to -1$ and $S_3 \to 0$. It is easy to see that, in this case, equation (1) reduces to the rigid body rotation equation. The opposite limiting case of weak interaction takes place when $S_2 \ll 1$ and $S_3 \ll 1$. However, it is important to keep in mind that the quasi-stationary formalism is applicable to the systems whose age exceeds the crust–core interaction characteristic time-scale t_v which is greater, the weaker is the interaction.

In order to calculate S_2 and S_3 for the particular case one should start from local form of conservation laws. Equations (2) and (3) can be combined in the equation for the momentum density $\boldsymbol{J} = \rho\boldsymbol{v}$:

$$\partial_t \boldsymbol{J} + \boldsymbol{e}_i \nabla_j \Pi^{ij} = -\rho\nabla\Phi, \tag{59}$$

where $\Pi^{ij} = \rho v^i v^j + P\delta^{ij} - \pi^{ij}$. Multiplying equation (59) by $\boldsymbol{r}\times$ and integrating the result over the spherical cavity, one obtains equation (56) in which

$$\boldsymbol{M}_{\rm core} = \int [\boldsymbol{r} \times \boldsymbol{J}]{\rm d}V \tag{60}$$

and

$$\begin{aligned}\boldsymbol{N} &= -\oint\limits_{r=r_c} [\boldsymbol{r} \times \boldsymbol{J}](\boldsymbol{v} \cdot {\rm d}\boldsymbol{S}) + \oint\limits_{r=r_c} \pi^{ij}[\boldsymbol{r} \times \boldsymbol{e}_i](\boldsymbol{e}_j \cdot {\rm d}\boldsymbol{S}) \\ &= \oint\limits_{r=r_c} \pi^{ij}[\boldsymbol{r} \times \boldsymbol{e}_i](\boldsymbol{e}_j \cdot \boldsymbol{e}_r){\rm d}S. \end{aligned} \tag{61}$$

The first integral in expression (61) equals to zero because $v_r = 0$ at the surface.

The main contribution in interaction torque (61) comes from the derivatives of $\boldsymbol{q}_{(l)}$ with respect to ξ. Other terms are less by the factor $E^{1/2}$ and they can be neglected. Taking this into account and

using expression for viscous tensions tensor (25), one can rewrite expression (61) in the following form:

$$\boldsymbol{N} \approx -E^{1/2}\dot{\Omega}\rho^{(b)}r_{\rm c}^5\int_{4\pi}\partial_{\hat{\xi}}[\boldsymbol{e}_r\times\boldsymbol{q}_{(l)}]\,{\rm d}\Theta \tag{62}$$

$$= -E^{1/2}\dot{\Omega}\rho^{(b)}r_{\rm c}^5\int_{4\pi}([\boldsymbol{e}_r\times\boldsymbol{q}_{(\rm in)}]\mp\boldsymbol{q}_{(\rm in)})|\boldsymbol{e}_r\cdot\boldsymbol{e}_z|^{1/2}\,{\rm d}\Theta. \tag{63}$$

where $\mathrm{d}\Theta$ is the element of solid angle. The last expression is obtained with using expression (40). It is obvious that the axisymmetric 'parallel' flow does not contribute in S_2 and S_3. As for the 'perpendicular' current, the secondary flow gives an additional factor $E^{1/2}$. Thus, it is enough to substitute only solid rotation velocity field (53) into interaction torque expression (63). Integration gives

$$S_2 = -\frac{8\pi}{5}\frac{\rho^{(b)}r_{\rm c}^5}{I_{\rm core}}E^{1/2},\quad S_3 = \frac{40\pi}{21}\frac{\rho^{(b)}r_{\rm c}^5}{I_{\rm core}}E^{1/2}. \tag{64}$$

Coefficients S_2 and S_3 are of the order of $E^{1/2}$.

2.4 Equations of motion

Let us introduce a new orthonormal basis $(\boldsymbol{\varepsilon}_x, \boldsymbol{\varepsilon}_y, \boldsymbol{\varepsilon}_m)$ which is fixed in the crust such that $\boldsymbol{\varepsilon}_m$ is directed along the star magnetic moment $\boldsymbol{m}$. The position of angular velocity vector can be described by two angles: inclination angle χ and 'azimuthal' angle φ_Ω (see Fig. 2).

The external torque can be represented in the following form:

$$\boldsymbol{K} = K_0\left(\tilde{k}_\Omega\boldsymbol{e}_z + \tilde{k}_m\boldsymbol{\varepsilon}_m + \tilde{k}_\perp[\boldsymbol{e}_z\times\boldsymbol{\varepsilon}_m]\right), \tag{65}$$

where $\tilde{k}_\Omega$, $\tilde{k}_m$, $\tilde{k}_\perp$ are some dimensionless functions of χ, φ_Ω (and other possible variables specific for particular magnetosphere model), K_0 is the value of the torque acting on an aligned ($\chi = 0$) pulsar.

Substituting torque expressions (65) and (55) into equation (1) and solving it for $\dot{\boldsymbol{\Omega}}$, one can represent the result as three scalar equations describing pulsar braking, inclination angle evolution and torque-driven precession:

$$\dot{\Omega} = \frac{K_0}{I_{\rm tot}}\left(\tilde{k}_\Omega + \tilde{k}_m\cos\chi\right) \tag{66}$$

$$\dot{\chi} = -\frac{K_0}{\Omega}\frac{(I_{\rm crust}-S_2I_{\rm core})\tilde{k}_m - S_3I_{\rm core}\tilde{k}_\perp}{(I_{\rm crust}-S_2I_{\rm core})^2+S_3^2I_{\rm core}^2}\sin\chi, \tag{67}$$

$$\dot{\varphi}_\Omega = -\frac{K_0}{\Omega}\frac{(I_{\rm crust}-S_2I_{\rm core})\tilde{k}_\perp + S_3I_{\rm core}\tilde{k}_m}{(I_{\rm crust}-S_2I_{\rm core})^2+S_3^2I_{\rm core}^2}, \tag{68}$$

where $I_{\rm tot} = I_{\rm crust} + I_{\rm core}$.

The rigid-star approximation corresponds to limiting case $I_{\rm core} \to 0$ of equations (67) and (68):

$$\dot{\chi} = -\frac{K_0}{I_{\rm tot}\Omega}\tilde{k}_m\sin\chi, \tag{69}$$

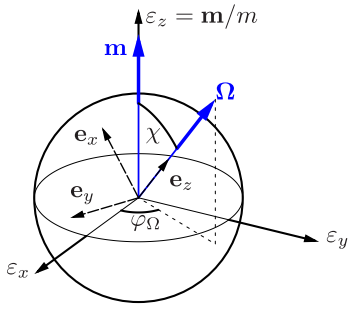

Figure 2. Vectors and coordinates used in Section 2.4.

$$\dot{\varphi}_\Omega = -\frac{K_0}{I_{\rm tot}\Omega}\tilde{k}_\perp. \tag{70}$$

Equation (66) does not change the form as it was argued in previous section. Note, however, that it does not mean that the braking should occur with the same rate. The right-hand side of equation (66) depends on χ and φ_Ω whose evolution is sensitive to the internal flows.

The presence of liquid core modifies the equations in two ways. First, the full moment of inertia $I_{\rm tot}$ in the denominator is replaced by the combinations of $(I_{\rm crust} - S_2I_{\rm core})$ and $S_3I_{\rm core}$ which are much less than $I_{\rm tot}$. If $|S_2|, S_3 \ll I_{\rm crust}/I_{\rm core}$, $I_{\rm tot}$ is replaced just by $I_{\rm crust}$. It leads to acceleration of angles evolution. Second, equation (67) contains $\tilde{k}_\perp$ (multiplied by S_3) which does not influence the inclination angle evolution in the case of rigid star (cf. Casini & Montemayor 1998). This effect becomes important when

$$S_3\tilde{k}_\perp \gtrsim \left(\frac{I_{\rm crust}}{I_{\rm core}} - S_2\right)\tilde{k}_m. \tag{71}$$

The precession formally is affected by $\tilde{k}_m$ through S_3 as well. However, this effect becomes comparable with $\tilde{k}_\perp$ if

$$S_3\tilde{k}_m \gtrsim \left(\frac{I_{\rm crust}}{I_{\rm core}} - S_2\right)\tilde{k}_\perp. \tag{72}$$

But since $\tilde{k}_\perp \sim 10^3\tilde{k}_m$, $I_{\rm crust}/I_{\rm core} \ll 1$ and $|S_2| \sim S_3 \ll 1$, this condition hardly can be satisfied. The torque-driven precession period is equal to

$$T_{\rm p} \approx \frac{\Omega I_{\rm crust}}{2\pi K_0\tilde{k}_\perp}. \tag{73}$$

It is much less than the inclination angle evolution time-scale.

3 THE EFFECTS OF COMPOSITION GRADIENT

In real neutron star the composition of the matter changes with depth. Therefore, the more realistic model should include equation

$$2[\boldsymbol{\Omega}\times\boldsymbol{u}] + \nabla\varkappa^{(1)} + y^{(0)}\nabla(\mu_{\rm c}^{(1)} - \mu_{\rm n}^{(1)}) = -[\dot{\boldsymbol{\Omega}}\times\boldsymbol{r}], \tag{74}$$

instead equation (42), where function $\varkappa$ is redefined as $\varkappa = \mu_{\rm n} + \Phi - \frac{1}{2}[\boldsymbol{\Omega}\times\boldsymbol{r}]^2$. Here, we also suppose the chemical equilibrium for unperturbed star ($m_{\rm n}\mu_{\rm n}^{(0)} = m_{\rm p}\mu_{\rm p}^{(0)} + m_{\rm e}\mu_{\rm e}^{(0)}$) and here and after we assume that $m_{\rm n} = m_{\rm p} + m_{\rm e}$. If one does not make the last assumption, an additional force proportional to $m_{\rm n} - m_{\rm p} - m_{\rm e}$ arises in equation (74). However, this force is the consequence of inconsistence of Newtonian hydrodynamics with reactions with non-conserved mass. It can be shown that in relativistic equation such force does not appear.

Now, in addition to $\varkappa^{(1)}$, there is another unknown function $\mu_{\rm c}^{(1)} - \mu_{\rm n}^{(1)}$. Hence, an additional equation is needed to the system to be closed. Continuity equation (43) can be split into two equations

$$\mathrm{div}\left(\rho_{\rm n}^{(0)}\boldsymbol{u}\right) = \Gamma_{\rm n}^{(1)}, \tag{75}$$

$$\mathrm{div}\left(\rho_{\rm c}^{(0)}\boldsymbol{u}\right) = -\Gamma_{\rm n}^{(1)}, \tag{76}$$

where the neutron creation rate $\Gamma_{\rm n}$ is proportional to the chemical potential difference (Haensel, Levenfish & Yakovlev 2000):

$$\Gamma_{\rm n}^{(1)} = \lambda_{\rm n}^{(0)}(\mu_{\rm c}^{(1)} - \mu_{\rm n}^{(1)}). \tag{77}$$

Combining equations (43) and (76), one can express this difference as a function of u_r:

$$(\mu_{\rm c}^{(1)} - \mu_{\rm n}^{(1)}) = -\frac{\rho^{(0)}}{\lambda_{\rm n}^{(0)}} \frac{{\rm d}y^{(0)}}{{\rm d}r} u_r, \tag{78}$$

and equation (74) takes the form

$$2[\boldsymbol{\Omega} \times \boldsymbol{u}] - y^{(0)} \nabla \left(\frac{\rho^{(0)}}{\lambda_{\rm n}^{(0)}} \frac{{\rm d}y^{(0)}}{{\rm d}r} u_r \right) + \nabla \varkappa^{(1)} = -[\dot{\boldsymbol{\Omega}} \times \boldsymbol{r}]. \tag{79}$$

It is more convenient to introduce a new variable $\mathfrak{H}$ instead $h^{(1)}$ in the following way:

$$\mathfrak{H} = \varkappa^{(1)} - y^{(0)} \frac{\rho^{(0)}}{\lambda_{\rm n}^{(0)}} \frac{{\rm d}y^{(0)}}{{\rm d}r} u_r. \tag{80}$$

It allows us to rewrite equation (79) in algebraic with respect to $\boldsymbol{u}$ form:

$$2[\boldsymbol{\Omega} \times \boldsymbol{u}] + g(r) u_r \boldsymbol{e}_r + \nabla \mathfrak{H} = -[\dot{\boldsymbol{\Omega}} \times \boldsymbol{r}], \tag{81}$$

where we have introduced function

$$g(r) = \frac{\rho^{(0)}}{\lambda_{\rm n}^{(0)}} \left(\frac{{\rm d}y^{(0)}}{{\rm d}r} \right)^2. \tag{82}$$

The neutron component turns to the charged and vice versa through the direct and modified Urca reactions. For neutron branch of modified Urca reaction $n + n \rightarrow n + p + e^- + \bar{\nu}_{\rm e}$ (Haensel, Levenfish & Yakovlev 2001)

$$\lambda_{\rm n} = 1.1 \times 10^{-14} R_{\rm f} \frac{m_{\rm p}^*}{m_{\rm p}} \left(\frac{m_{\rm n}^*}{m_{\rm n}} \right)^3 \left(\frac{n_{\rm e}}{n_0} \right)^{1/3} \times \left(\frac{T}{10^9\ {\rm K}} \right)^6 {\rm g}^2\ {\rm sm}^{-3}\ {\rm s}^{-1}\ {\rm erg}^{-1}. \tag{83}$$

For proton branch $n + p \rightarrow p + p + e^- + \bar{\nu}_{\rm e}$, $\lambda_{\rm n}$ is of the same order of magnitude. For direct Urca reaction $n \rightarrow p + e^- + \bar{\nu}_{\rm e}$ (Haensel et al. 2000)

$$\lambda_{\rm n} = 5.6 \times 10^{-8} R_{\rm f} \frac{m_{\rm p}^*}{m_{\rm p}} \frac{m_{\rm n}^*}{m_{\rm n}} \left(\frac{n_{\rm e}}{n_0} \right)^{1/3} \times \left(\frac{T}{10^9\ {\rm K}} \right)^4 {\rm g}^2\ {\rm sm}^{-3}\ {\rm s}^{-1}\ {\rm erg}^{-1} \tag{84}$$

Here, $m_{\rm n}^*$ and $m_{\rm p}^*$ are the effective masses of neutrons and protons, $R_{\rm f}$ is the factor describing the reduction of the reactions by proton superconductivity and neutron superfluidity. Note that our definition of $\lambda_{\rm n}$ differs from the one given by Haensel et al. by factor $m_{\rm n}^2$. It is easy to verify that $g(r)/\Omega$ is very large in all possible cases. So, as it follows from equation (81), any radial flow should be strongly damped by chemical composition gradient. It means that the angular momentum cannot be transferred into the crust by Ekman mechanism (cf. Abney & Epstein 1996) but only by viscous tensions. In this case, the boundary layer formalism developed in Section 2.2 is not applicable and, hence, we should return viscous force $\boldsymbol{f}_{\rm v}^{(1)}$ into the equations.

Since $u_r \ll u_\theta, u_\phi$, continuity equation (43) can be replaced by

$${\rm div}\boldsymbol{u} = 0. \tag{85}$$

Substituting equation (85) into viscous tensions tensor expression (24), one can exclude the bulk viscosity from the consideration. Let us also assume that

$$\eta = {\rm const}, \quad \rho = {\rm const}. \tag{86}$$

It is, of course, not quite realistic. However, as it will be seen, the result practically does not change if one relax this assumption.

So, now the rotating neutron star described by 'Navier–Stokes' equation

$$-\nu^{(0)} \nabla^2 \boldsymbol{u} + 2[\boldsymbol{\Omega} \times \boldsymbol{u}] + g(r) u_r \boldsymbol{e}_r + \nabla \mathfrak{H} = -[\dot{\boldsymbol{\Omega}} \times \boldsymbol{r}], \tag{87}$$

continuity equation (85), equation (1), and boundary condition

$$\boldsymbol{u}_{r=r_{\rm c}} = 0. \tag{88}$$

Interaction torque $\boldsymbol{N}$ is calculated with the formula (61).

As before linear approximation allows us to consider the flows proportional to $\dot{\Omega}_{||}$ and $\dot{\Omega}_{\perp}$ separately. The 'parallel' flow velocity field has the form

$$\boldsymbol{u}_{||} \approx -\boldsymbol{e}_\phi \frac{1}{10} \frac{\dot{\Omega}_{||}}{\Omega} E^{-1} \left(1 - \frac{r^2}{r_{\rm c}^2} \right) r \sin\theta. \tag{89}$$

This flow is almost azimuthal (poloidal flow is of the order of $\Omega/g(r)$ and it obviously can be neglected). In contrast to the case of Ekman pumping, where the azimuthal component of $\boldsymbol{u}$ is proportional to $E^{-1/2}$, here it is much larger and has the order of magnitude $\sim E^{-1}$.

Substitution of expression (89) into (61) gives

$$\boldsymbol{N} = -\boldsymbol{e}_z \dot{\Omega}_{||} \rho^{(b)} \frac{8\pi}{15} r_{\rm c}^5 = -\boldsymbol{e}_z I_{\rm core} \dot{\Omega}_{||}. \tag{90}$$

Here, calculating the moment of inertia, we have used the formula for the spherical body of constant density

$$I_{\rm core} = \frac{8\pi}{15} r_{\rm c}^5 \rho^{(b).} \tag{91}$$

It is consistent with assumption (86). It is exactly what we should obtain according to the arguments from Section 2.3. These arguments ensure that despite the fact that the relaxation of the constant viscosity assumption leads to more complicated expression for $\boldsymbol{u}$, the torque (90) remains the same.

The velocity field of 'perpendicular' flow can be represented in the following form:

$$\boldsymbol{u}_{\perp} \approx \frac{\dot{\Omega}_{\perp}}{\Omega} Re \left\{ U(r) (\boldsymbol{e}_\phi \cos\theta - i \boldsymbol{e}_\theta) {\rm e}^{{\rm i}\phi} \right\}, \tag{92}$$

$$U(r) = i r_{\rm c} \left(\frac{r}{r_{\rm c}} - \frac{j_1(kr)}{j_1(kr_{\rm c})} \right), \tag{93}$$

$$k = \frac{1+i}{\sqrt{2}} \frac{E^{-1/2}}{r_{\rm c}}, \tag{94}$$

where

$$j_1(x) = \frac{1}{x} \left(\frac{\sin(x)}{x} - \cos(x) \right) \tag{95}$$

is a spherical Bessel function.

In almost the entire volume of star core the flow has the form of a rigid rotation coinciding with (53). Only in a thin layer $\sim E^{1/2} r_{\rm c}$ adjustment to the crust velocity occurs. Note that whereas the braking of the star causes the flow which velocity profile is the smooth function of r, here the boundary layer takes place. The thickness of this layer is comparable in scale with the Ekman layer.

The origin of this difference was already discussed in Section 2.2. In the case of 'parallel' flow, the 'force' $[\dot{\boldsymbol{\Omega}}_{||} \times \boldsymbol{r}]$ causes the angular momentum flux directed away from the rotational axis in the whole bulk of the core. Since radial flows are damped, the angular momentum can only diffuse by viscous tensions. This requires the differential rotation of the core. In the case of 'perpendicular' flow, the 'external force' $[\dot{\boldsymbol{\Omega}}_{\perp} \times \boldsymbol{r}]$ is balanced by Coriolis force and the angular momentum flux does not appear in the bulk of the core. Therefore, in the quasi-stationary regime the rotation is rigid.

Only near the crust–core interface, where the flow should adjust to the boundary condition, the differential rotation (and the angular momentum flux) takes place.

Since the 'perpendicular' flow depends on η only in this layer, in fact, assumption (86) should be satisfied only in this layer (but not in the whole core) for the solution to be appropriate.

Substituting expression (92) into (61), one can obtain

$$S_2 = -\frac{8\pi\rho^{(b)}r_c^5}{3\sqrt{2}I_{\rm core}}E^{1/2},\quad S_3 = \frac{8\pi\rho^{(b)}r_c^5}{3\sqrt{2}I_{\rm core}}E^{1/2}. \tag{96}$$

Here, we have kept only the terms containing the lowest power of E. This power equals to 1/2. Despite the fact that for the time-dependent problem the relaxation through the viscous tensions is much less effective (characteristic time-scale $\sim(\Omega E)^{-1}$; Greenspan 1990), for the quasi-stationary problem the crust–core interaction coefficients are of the same order of magnitude as coefficients (64).

One thing should be pointed here. The centrifugal force which we have neglected makes the equilibrium composition depend on Ω. Due to braking and finite reaction rate, strictly speaking, even in the hydrostatic approximation there is no chemical equilibrium (Reisenegger 1995). It gives rise to an additional force $y^{(1)}\nabla(\mu_c^{(0)} - \mu_n^{(0)})$ acting in the same direction as the flow damped force. However, this additional term cannot change the situation because it is quadratically small $\sim \dot{\Omega}^2$. So, this effect can be ignored in our problem.

4 THE EFFECTS OF NEUTRON SUPERFLUIDITY

It is widely believed that the protons in some region of neutron star core should be in superconductive state as well as the neutrons should be in superfluid state (Yakovlev et al. 1999). The proton superconductivity damps nuclear reactions and changes different kinetic coefficients.

The effects of neutron superfluidity is more complicated. It causes the appearance of an additional hydrodynamical degree of freedom $\boldsymbol{v}_s$ which is related with the moving of superfluid neutrons. The system of two-fluid hydrodynamical equations can be formulated in the following form (Khalatnikov 2000; Mendell 1991)

$$\partial_t \boldsymbol{v}_s + (\boldsymbol{v}_s\cdot\nabla)\boldsymbol{v}_s + \nabla(\mu_n + \Phi) = \boldsymbol{f}_{\rm int} + \boldsymbol{f}_{\rm vs}, \tag{97}$$

$$\partial_t \boldsymbol{J} + \boldsymbol{e}_i\nabla_k\Pi^{ik} = -\rho\nabla\Phi, \tag{98}$$

$$\partial_t\rho + \mathrm{div}\,\boldsymbol{J} = 0, \tag{99}$$

$$\Phi(\boldsymbol{r}) = -G\int\frac{\rho(\boldsymbol{r}')}{|\boldsymbol{r}-\boldsymbol{r}'|}\,\mathrm{d}^3r'. \tag{100}$$

Here, $\boldsymbol{J}$ and Π^{ik} are the full mass current density and momentum flux density tensor, $\boldsymbol{f}_{\rm int}$ is the force per unit mass describing the interaction of superfluid neutrons with the rest matter of neutron star core, $\boldsymbol{f}_{\rm vs}$ is the superfluid neutron viscosity force.

Strictly speaking, superfluid flows are always potential. Therefore, in addition to equation (97), velocity field $\boldsymbol{v}_s$ should satisfy equation curl $\boldsymbol{v}_s = 0$. It means, for example, that the rigid rotation $\boldsymbol{u}_s = \boldsymbol{\Omega}\times\boldsymbol{r}$ cannot take place for superfluids. However, this kind of liquids can rotate by forming an array of vortices (Tilley & Tilley 1990). If the scales of considered problem are much larger that the intervortex space, it is convenient to use the smooth-averaged hydrodynamics (Khalatnikov 2000; Baym & Chandler 1983; Mendell 1991) The basic idea is that the discrete array of vortices is replaced by smooth field $\omega_s = \omega_s\boldsymbol{e}_v$, where

$$\omega_s = \frac{2\pi\hbar}{2m_n}n_v, \tag{101}$$

$\boldsymbol{e}_v$ is the unit vector pointing the vortices orientation and n_v is the number of vortices per unit area. The velocity field $\boldsymbol{v}_s$ is introduced through the equation

$$\boldsymbol{\omega}_s = \mathrm{curl}\ \boldsymbol{v}_s. \tag{102}$$

The superfluid neutrons do not interact with the rest matter directly but do it with mediation of vortices. This kind of interaction is called the mutual friction and described by force (Hall & Vinen 1956)

$$\boldsymbol{f}_{\rm int} = \beta'\boldsymbol{\omega}_s\times(\boldsymbol{v}_s - \boldsymbol{v}_c) + \beta\boldsymbol{e}_v\times[\boldsymbol{\omega}_s\times(\boldsymbol{v}_s - \boldsymbol{v}_c)], \tag{103}$$

where β and β' are the coefficients determined by the particular mutual friction mechanism. Note that the flows components along the vortices do not participate in mutual friction interaction.

In the framework of two-fluid approximation

$$\boldsymbol{J} = \rho_s\boldsymbol{v}_s + \rho_{ex}\boldsymbol{v}_c + \rho_c\boldsymbol{v}_c, \tag{104}$$

$$\Pi^{ij} = \rho_s v_s^i v_s^j + \rho_{ex}v_c^i v_c^j + \rho_c v_c^i v_c^j + P\delta^{ij} - \pi^{ij}, \tag{105}$$

where ρ_s and ρ_{ex} are the mass densities of the superfluid neutrons and neutron thermal excitations, respectively, $\rho_n = \rho_s + \rho_{ex}$ (Khalatnikov 2000), $\boldsymbol{v}_c$ is the velocity field of the charged component (neutron excitation are assumed to move together with the charged component), π^{ij} as before is the dissipative part of Π^{ij}.

Multiplying equation (97) by ρ_s, subtracting the result from equation (98) and using (99) and (5), one can obtain

$$\partial_t\boldsymbol{v}_c + (\boldsymbol{v}_c\cdot\nabla)\boldsymbol{v}_c + \nabla(\mu_c + \Phi) + y'\nabla(\mu_n - \mu_c) = -\frac{\rho_s}{\rho_c+\rho_{ex}}\boldsymbol{f}_{\rm int} + \boldsymbol{f}_{\rm vc} + \frac{Q_s}{\rho_c+\rho_{ex}}(\boldsymbol{v}_c - \boldsymbol{v}_s), \tag{106}$$

where $y' = \rho_{ex}/(\rho_c + \rho_{ex})$,

$$\boldsymbol{f}_{\rm vc} = \boldsymbol{e}_i\frac{1}{\rho_c+\rho_{ex}}\frac{\partial}{\partial r^k}\pi^{ik} - \frac{\rho_s}{\rho_c+\rho_{ex}}\boldsymbol{f}_{\rm vs}. \tag{107}$$

and

$$Q_s = \partial_t\rho_s + \mathrm{div}\,(\rho_s\boldsymbol{v}_s). \tag{108}$$

Reproducing all simplifications from Sections 2.1, 2.2 and 3, one can obtain the following linear quasi-stationary equations:

$$2[\boldsymbol{\Omega}\times\boldsymbol{u}_s] + \nabla\varkappa_s^{(1)} = -[\dot{\boldsymbol{\Omega}}\times\boldsymbol{r}] + \boldsymbol{f}_{\rm int}^{(1)} + \boldsymbol{f}_{\rm vs}^{(1)}, \tag{109}$$

$$2[\boldsymbol{\Omega}\times\boldsymbol{u}_c] + \nabla\varkappa_c^{(1)} + y'^{(0)}\nabla(\mu_n^{(1)} - \mu_c^{(1)}) = -[\dot{\boldsymbol{\Omega}}\times\boldsymbol{r}] - \frac{\rho_c^{(0)}}{\rho_c^{(0)}+\rho_{ex}^{(0)}}\boldsymbol{f}_{\rm int}^{(1)} + \boldsymbol{f}_{\rm vc}^{(1)}, \tag{110}$$

where $\varkappa_s^{(1)} = \mu_n^{(1)} + \Phi^{(1)}$ and $\varkappa_c^{(1)} = \mu_c^{(1)} + \Phi^{(1)}$. Two continuity equations also can be introduced (cf. Section 3):

$$\mathrm{div}(\rho_s^{(0)}\boldsymbol{u}_s + \rho_{ex}^{(0)}\boldsymbol{u}_c) = \lambda_n^{(0)}(\mu_c^{(1)} - \mu_n^{(1)}), \tag{111}$$

$$\mathrm{div}(\rho_c^{(0)}\boldsymbol{u}_c) = -\lambda_n^{(0)}(\mu_c^{(1)} - \mu_n^{(1)}). \tag{112}$$

In this paper, we will consider only the strong superfluidity limit, when the terms containing ρ_{ex} and λ_n are negligibly small. In this case, we have two fluids each of which is characterized by own mass density, own velocity field and own 'chemical potential'. The

composition gradient does not prevent radial flows and the Ekman pumping again becomes possible. Thus, for bulk of the core we can use 'inviscid' equations

$$2[\boldsymbol{\Omega}\times\boldsymbol{u}_{\rm s}]+\nabla\varkappa_{\rm s}^{(1)}=-[\dot{\boldsymbol{\Omega}}\times\boldsymbol{r}]+\boldsymbol{f}_{\rm int}^{(1)}, \tag{113}$$

$$2[\boldsymbol{\Omega}\times\boldsymbol{u}_{\rm c}]+\nabla\varkappa_{\rm c}^{(1)}=-[\dot{\boldsymbol{\Omega}}\times\boldsymbol{r}]-\frac{\rho_{\rm n}^{(0)}}{\rho_{\rm c}^{(0)}}\boldsymbol{f}_{\rm int}^{(1)}, \tag{114}$$

$$\mathrm{div}(\rho_{\rm c}^{(0)}\boldsymbol{u}_c)=0, \tag{115}$$

$$\mathrm{div}(\rho_{\rm s}^{(0)}\boldsymbol{u}_{\rm s})=0. \tag{116}$$

Let us first consider the situation when the region of neutron superfluidity extends up to the crust. In this case, we should specify the boundary conditions at the crust–core interface. Here, we consider only the weak mutual friction ($\beta,\ \beta'\ll 1$) which is expected for neutron star matter. It means that the mutual friction force is much smaller than the viscous force in the boundary layer, namely $\tilde{f}_{\rm v}\sim 1$ and $\tilde{f}_{\rm mf}\sim\max(\beta,\ \beta')$ there (van Eysden & Melatos 2013). This fact allows us to formulate the boundary conditions for $\boldsymbol{u}_{\rm c}$ and $\boldsymbol{u}_{\rm s}$ separately. The charged component velocity field $\boldsymbol{u}_{\rm c}$ should satisfy the Ekman boundary condition (44). As for the neutrons, the superfluids have no shear viscosity (Khalatnikov 2000), thus, superfluid component should satisfy ordinary no-penetration condition:

$$\left(\rho_{\rm s}^{(0)}(\boldsymbol{e}_r\cdot\boldsymbol{u}_{\rm s})\right)_{r=r_{\rm c}}=0. \tag{117}$$

After linearization, the mutual friction force takes the form:

$$\begin{aligned}\boldsymbol{f}_{\rm int}^{(1)}&=2\Omega\beta'^{(0)}\boldsymbol{e}_z\times(\boldsymbol{u}_{\rm s}-\boldsymbol{u}_{\rm c})\\&\quad+2\Omega\beta^{(0)}\boldsymbol{e}_z\times[\boldsymbol{e}_z\times(\boldsymbol{u}_{\rm s}-\boldsymbol{u}_{\rm c})]\,.\end{aligned} \tag{118}$$

Here, we have taken into account that $\boldsymbol{\omega}_{\rm s}=2\boldsymbol{\Omega}+\mathrm{curl}\boldsymbol{u}_{\rm n}$ and

$$\boldsymbol{e}_{\rm v}\approx\boldsymbol{e}_z-\boldsymbol{e}_z\times\left[\boldsymbol{e}_z\times\frac{\mathrm{curl}\boldsymbol{u}_{\rm s}}{2\Omega}\right]. \tag{119}$$

The substitution of expresion (118) into equations (113) and (114) gives

$$\begin{aligned}&2\Omega[\boldsymbol{e}_z\times\boldsymbol{u}_{\rm s}]+2\Omega\beta'^{(0)}[\boldsymbol{e}_z\times\delta\boldsymbol{u}]\\&+2\Omega\beta^{(0)}\boldsymbol{e}_z\times[\boldsymbol{e}_z\times\delta\boldsymbol{u}]+\nabla\varkappa_{\rm s}=-[\dot{\boldsymbol{\Omega}}\times\boldsymbol{r}],\end{aligned} \tag{120}$$

$$\begin{aligned}&2\Omega[\boldsymbol{e}_z\times\boldsymbol{u}_{\rm c}]-2\Omega\beta'^{(0)}\frac{\rho_{\rm s}^{(0)}}{\rho_{\rm c}^{(0)}}[\boldsymbol{e}_z\times\delta\boldsymbol{u}]\\&-2\Omega\beta^{(0)}\frac{\rho_{\rm s}^{(0)}}{\rho_{\rm c}^{(0)}}\boldsymbol{e}_z\times[\boldsymbol{e}_z\times\delta\boldsymbol{u}]+\nabla\varkappa_{\rm c}=-[\dot{\boldsymbol{\Omega}}\times\boldsymbol{r}],\end{aligned} \tag{121}$$

where $\delta\boldsymbol{u}=\boldsymbol{u}_{\rm c}-\boldsymbol{u}_{\rm s}$. These equations together with equations (115) and (116) allow us to express $\boldsymbol{u}_{\rm c}$ and $\boldsymbol{u}_{\rm s}$ as functions of $\dot{\boldsymbol{\Omega}}$.

Let us first discuss the 'perpendicular' flow. It can be verified that

$$\begin{aligned}\boldsymbol{u}_{c\perp}&=\left[\boldsymbol{e}_z\times\frac{\dot{\boldsymbol{\Omega}}}{\Omega}\right]\times\boldsymbol{r}\\&\quad-\boldsymbol{e}_z\frac{\dot{\Omega}_\perp}{4\Omega}E^{1/2}\frac{\rho_{cb}^{(0)}}{\rho_{\rm c}^{(0)}}\left(\frac{r_{\rm c}}{z_b}\right)^{3/2}\left(3\varpi\sin\phi+\frac{r_{\rm c}}{z_b}\varpi\cos\phi\right),\end{aligned} \tag{122}$$

$$\boldsymbol{u}_{s\perp}=\left[\boldsymbol{e}_z\times\frac{\dot{\boldsymbol{\Omega}}}{\Omega}\right]\times\boldsymbol{r}, \tag{123}$$

$$\varkappa_{c\perp}=\varkappa_{s\perp}=-\dot{\Omega}_\perp z\varpi\sin\phi, \tag{124}$$

satisfy all equations and boundary conditions. So, both components rigidly rotate with the same angular velocity (52). The secondary flow is generated only in charged component. It has the structure similar to the case of ordinary fluid discussed in Section 2.2. The charged component secondary flow does not influence on the superfluid component in the linear approximation because it is directed along the neutron vortices. The same structure of the secondary flow gives almost the same crust–core interaction coefficients S_2 and S_3. One just needs to replace $\rho^{(b)}$ by $\rho_{\rm c}^{(b)}$ in coefficients (64):

$$S_2=-\frac{8\pi}{5}\frac{\rho_{\rm c}^{(b)}r_{\rm c}^5}{I_{\rm core}}E^{1/2},\quad S_3=\frac{40\pi}{21}\frac{\rho_{\rm c}^{(b)}r_{\rm c}^5}{I_{\rm core}}E^{1/2}. \tag{125}$$

The 'parallel' flow is more complicated. For the case $\dot{\boldsymbol{\Omega}}=\dot{\boldsymbol{\Omega}}_{||}$, velocity fields have the forms:

$$\begin{aligned}\boldsymbol{u}_{s||}&=-(\psi_{\rm s}+K\delta\psi)\frac{\dot{\Omega}_{||}}{2\Omega}\varpi\boldsymbol{e}_\phi-(1+A\delta\psi)\frac{\dot{\Omega}_{||}}{2\Omega}\varpi\boldsymbol{e}_\varpi\\&\quad+\boldsymbol{e}_z\frac{\dot{\Omega}_{||}}{2\Omega\rho_{\rm s}^{(0)}}\int_0^z\left[\frac{1}{\varpi}\frac{\partial}{\partial\varpi}\varpi^2\left(\rho_{\rm n}^{(0)}+\rho_{\rm s}^{(0)}A\delta\psi\right)\right]\mathrm{d}z'\\&\quad+\frac{H_{\rm s}(\varpi,\phi)}{\rho_{\rm s}^{(0)}}\boldsymbol{e}_z,\end{aligned} \tag{126}$$

$$\begin{aligned}\boldsymbol{u}_{c||}&=-\left(\psi_{\rm c}-K\frac{\rho_{\rm s}^{(0)}}{\rho_{\rm c}^{(0)}}\delta\psi\right)\frac{\dot{\Omega}_{||}}{2\Omega}\varpi\boldsymbol{e}_\phi\\&\quad-\left(1-A\frac{\rho_{\rm s}^{(0)}}{\rho_{\rm c}^{(0)}}\delta\psi\right)\frac{\dot{\Omega}_{||}}{2\Omega}\varpi\boldsymbol{e}_\varpi\\&\quad+\boldsymbol{e}_z\frac{\dot{\Omega}_{||}}{2\Omega\rho_{\rm c}^{(0)}}\int_0^z\left[\frac{1}{\varpi}\frac{\partial}{\partial\varpi}\varpi^2\left(\rho_{\rm c}^{(0)}-\rho_{\rm s}^{(0)}A\delta\psi\right)\right]\mathrm{d}z'\\&\quad+\frac{H_{\rm c}(\varpi,\phi)}{\rho_{\rm c}^{(0)}}\boldsymbol{e}_z,\end{aligned} \tag{127}$$

where $H_{\rm s}$ and $H_{\rm c}$ are the functions of ϖ and ϕ determined by the boundary conditions, functions ψ_α are introduced through the equation

$$\varkappa_{\alpha||}=-\dot{\Omega}_{||}\int_0^\varpi\psi_\alpha(\varpi')\varpi'\,\mathrm{d}\varpi', \tag{128}$$

and we have denoted the difference $\psi_{\rm c}-\psi_{\rm n}$ by $\delta\psi$. The notations A and K are used for the following combinations:

$$A=\frac{\left[\rho_{\rm c}^{(0)}\right]^2\beta^{(0)}}{\left[\beta^{(0)}\rho^{(0)}\right]^2+\left[\rho_{\rm c}^{(0)}-\beta'^{(0)}\rho^{(0)}\right]^2}, \tag{129}$$

$$K=\frac{\rho_{\rm c}^{(0)}}{\rho^{(0)}}-\frac{\rho_{\rm c}^{(0)}}{\rho^{(0)}}\frac{\left[\rho_{\rm c}^{(0)}\right]^2-\rho_{\rm c}^{(0)}\rho^{(0)}\beta'^{(0)}}{\left[\beta^{(0)}\rho^{(0)}\right]^2+\left[\rho_{\rm c}^{(0)}-\beta'^{(0)}\rho^{(0)}\right]^2}. \tag{130}$$

The application of boundary condition (117) to $\boldsymbol{u}_{s||}$ gives

$$\delta\psi=-\left[\int_0^{z_b}\rho_{\rm n}^{(0)}\,\mathrm{d}z'\right]\left[\int_0^{z_b}A\rho_{\rm n}^{(0)}\,\mathrm{d}z'\right]^{-1},\quad H_{\rm s}=0. \tag{131}$$

Finally, using boundary condition (44), one can determine $\psi_{\rm c}$:

$$\begin{aligned}\psi_{\rm c}(\varpi)&=\left(K\frac{\rho_{\rm s}^{(0)}}{\rho_{\rm c}^{(0)}}\right)_{r=r_{\rm c}}\delta\psi(\varpi)\\&\quad+\left(\frac{|\boldsymbol{e}_r\cdot\boldsymbol{e}_z|}{E}\right)^{1/2}\frac{2J_\rho}{\rho_{sb}^{(0)}r_{\rm c}}-\frac{1}{\rho_{sb}^{(0)}r_{\rm c}}\frac{1}{\varpi}\frac{\mathrm{d}}{\mathrm{d}\varpi}\left(\varpi^2J_\rho\right)-\frac{r_{\rm c}}{z_b}\end{aligned} \tag{132}$$

$$\approx\left(K\frac{\rho_{\rm s}^{(0)}}{\rho_{\rm c}^{(0)}}\right)_{r=r_{\rm c}}\delta\psi(\varpi)+\left(\frac{|\boldsymbol{e}_r\cdot\boldsymbol{e}_z|}{E}\right)^{1/2}\frac{2J_\rho}{\rho_{sb}^{(0)}r_{\rm c}}, \tag{133}$$

and $H_{\rm c}=0$. Here,

$$J_\rho=\int_0^{z_b}(\rho_{\rm c}^{(0)}+\rho_{\rm s}^{(0)})\,\mathrm{d}z'. \tag{134}$$

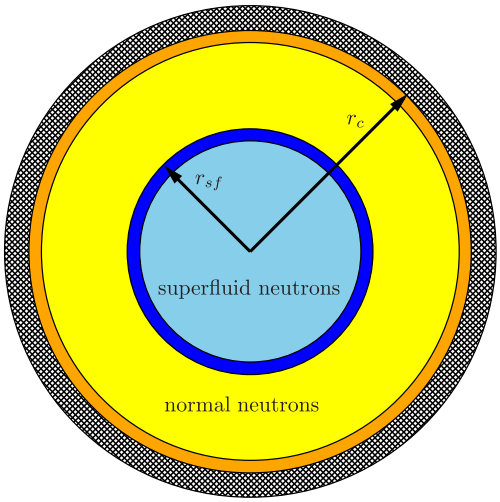

Figure 3. The structure of neutron star interior.

Both fluids rotate differentially. The charged component rotates with angular velocity

$$\boldsymbol{\Omega} - \frac{\dot{\boldsymbol{\Omega}}_{||}}{2\Omega}\left(\psi_{\rm c} - K\frac{\rho_{\rm n}^{(0)}}{\rho_{\rm c}^{(0)}}\delta\psi\right) \tag{135}$$

which is slightly larger than $\boldsymbol{\Omega}$. The superfluid component rotates with angular velocity

$$\boldsymbol{\Omega} - \frac{\dot{\boldsymbol{\Omega}}_{||}}{2\Omega}\left(\psi_{\rm c} - \delta\psi + K\delta\psi\right) \tag{136}$$

which is slightly larger than angular velocity of the charged component.

The neutron and charged secondary flows are different as well. However, the full poloidal mass current

$$\rho_{\rm c}^{(0)}\boldsymbol{u}_{\rm c} + \rho_{\rm s}^{(0)}\boldsymbol{u}_{\rm s} = \rho^{(0)}\frac{\dot{\Omega}_{||}}{2\Omega}\boldsymbol{e}_{\varpi}\varpi + \boldsymbol{e}_z\frac{\dot{\Omega}_{||}}{2\Omega}\int_0^z \frac{1}{\varpi}\frac{\partial}{\partial\varpi}\left(\varpi^2\rho^{(0)}\right)\,{\rm d}z' \tag{137}$$

coincides with the case of ordinary fluid. It is an expected result because this current should carry the angular momentum such that the corresponding coefficient S_1 will be equal to unity.

In real neutron star, at least if it is not too old, the region of core neutron superfluidity does not reach its crust. There is the interlayer of normal neutrons (see Fig. 3). So, the flow appearing as a reaction on $\dot{\boldsymbol{\Omega}}$ has a complex structure in the general case. However, the long-term dynamics of the star rotation can be understood without knowing of exact form of the flow.

There are two key points. First, as it was argued in Section 2.3, as long as the flow in the core is quasi-stationary coefficient S_1 should be equal to unity. Thus, there is no need to know the exact structure of 'parallel' flow if one only wants to calculate $\boldsymbol{N}$. The second point is that the 'perpendicular' flow has the form of rigid rotation with angular velocity (52) in almost the entire volume of star core. The flow significantly differs from rigid body rotation only in the thin layers where the velocity field adjusts to the boundary condition.

Two boundary layers should take place in general case (see. Fig. 3). The first is located near the crust–core interface. The second arises in the region where the neutron superfluidity breaks. Although we do not know the exact structure of the second boundary layer, we can be sure that its influence decreases towards the crust with characteristic scale $\sim E^{1/2}r_{\rm c}$. It means that the crust–core boundary layer does not feel the presence of superfluid neutrons in the depth of the core. So, the results of Section 3 remain valid and the core reaction is described by coefficients (96) until neutron superfluidity reach the crust. When this happens, the coefficients reduce to values (125). It should be noted that, calculating coefficients (125), we do not take into account any possible vortex–crust interaction which, in principal, can significantly change the result.

5 EXTERNAL ELECTROMAGNETIC TORQUE

The simplest magnetosphere model treats a pulsar as a magnetized sphere rotating in vacuum. In the case of slow rotation ($r_{\rm ns}\Omega/c \ll 1$), the torque equals to (Davis & Goldstein 1970; Melatos 2000)

$$\boldsymbol{K} = \frac{2\Omega^2}{3c^3}\boldsymbol{m}\times[\boldsymbol{m}\times\boldsymbol{\Omega}] + \frac{\zeta}{r_{\rm ns}c^2}(\boldsymbol{m}\cdot\boldsymbol{\Omega})[\boldsymbol{\Omega}\times\boldsymbol{m}], \tag{138}$$

where $\boldsymbol{m}$ is the neutron star magnetic moment. The two terms in equation (138) have different physical origin. The first term is the radiation reaction torque. It equals (with minus) to the angular momentum carried away by the electromagnetic wave per unit time. The second term is the so-called anomalous torque. It is caused by inertia of the near-zone electromagnetic field. Here, ζ is the constant $\sim$1 determined by the exact fields configuration. Note that the anomalous torque larger than the first term in expression (138) approximately by factor

$$\frac{c}{\Omega r_{\rm ns}} = 4.7\times10^3\left(\frac{P}{1\,{\rm s}}\right)\left(\frac{r_{\rm ns}}{10\,{\rm km}}\right)^{-1}. \tag{139}$$

It means that $\tilde{k}_\perp \gg \tilde{k}_\Omega,\ \tilde{k}_m$.

Real neutron stars do not rotate in vacuum. They are surrounded by large magnetosphere. Strictly speaking, the torque acting on a neutron star can be calculated only by using a self-consistent theory of the magnetosphere which despite the achieved progress is far from complete at present (Spitkovsky 2008). For example, Beskin, Gurevich & Istomin (1983) have shown that in some special case the magneto-dipolar radiation should absent at all. Beskin et al. (2013) have argued that the magneto-dipolar radiation can absent in general case. However, in any case, the corrections to the magnetic field due to the presence of the magnetosphere is small near the star (where the most of angular momentum is contained) and the electric field generated by rotation is of the order of $\frac{\Omega r}{c}B$ (Beskin 2009). It allows us to suppose that the anomalous torque is comparable with the one calculated under the vacuum approximation. Particular fields configuration describes by constant ζ.

In our calculations, we will use two different torques causing relatively slow inclination angle evolution. The first one is the model torque proposed by Barsukov et al. (2009)

$$\boldsymbol{K}_{\rm BPT} = \frac{2}{3}\frac{m^2\Omega^3}{c^3}\left(\boldsymbol{\varepsilon}_m\left(1-\alpha\left(\chi,\varphi_\Omega\right)\right)\cos\chi - \boldsymbol{e}_z + \zeta\frac{c}{\Omega r_{\rm ns}}[\boldsymbol{e}_z\times\boldsymbol{\varepsilon}_m]\cos\chi\right). \tag{140}$$

The authors have argued that the presence of small-scale magnetic field at the star surface causes the modulation of magnetospheric currents and, consequently, the modulation of angular momentum losses during star precision. These processes are described by depending on angles function $\alpha\left(\chi,\varphi_\Omega\right) \sim 1$. In order to investigate

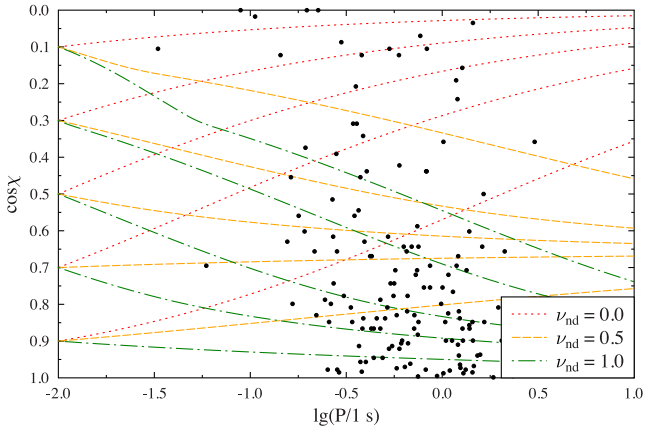

Figure 4. The $\cos\chi - P$ trajectories for pulsars with initial period $P_0 = 10$ ms and different non-dipolarity parameters ν_{nd} and initial inclination angles evaluating under the action of BPT-torque. Observational data shown by dots are taken from Rankin (1993).

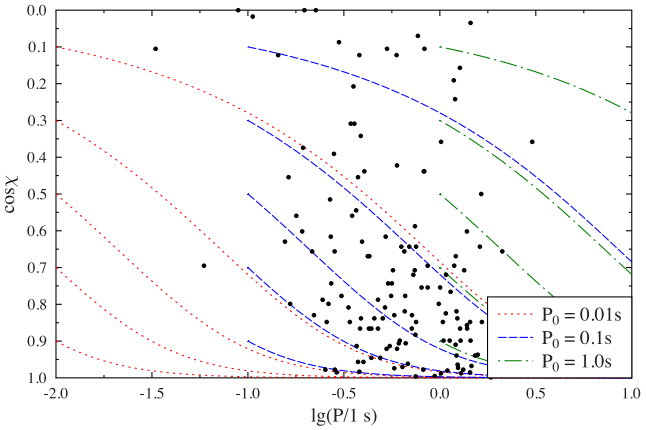

Figure 5. The $\cos\chi - P$ trajectories for pulsars with different initial periods and initial inclination angles evaluating under the action of PTL-torque. Observational data shown by dots are taken from Rankin (1993).

the secular rotation evolution, it is possible to use equations (67) and (68) averaged over T_p. One just needs to replace $\alpha(\chi, \varphi_\Omega)$ by

$$\bar{\alpha}(\chi) = \frac{1}{2\pi}\int_0^{2\pi} \alpha(\chi, \varphi_\Omega)\, \mathrm{d}\varphi_\Omega, \tag{141}$$

where $\bar{\alpha}$ depends on the non-dipolarity parameter $\nu_{nd} = B_{sc}/B_{dp}$, B_{sc} and B_{dp} are the strengths of the small-scale and dipolar magnetic fields at the polar caps. Barsukov et al. have argued that the solution of equation $\bar{\alpha}(\chi_{eq}) = 1$ can exist and should be a stable equilibrium inclination angle.

The direction of the evolution and equilibrium inclination angle depend on ν_{nd}. The inclination angle trajectories of rigid neutron star under the action of torque (140) for different values of ν_{nd} are given in Fig. 4. The pulsars with pure dipole field evolves to orthogonal state. The pulsars with $\nu_{nd} = 1$ aim to become coaxial. Non-dipolarity parameter $\nu_{nd} = 0.5$ corresponds to equilibrium angle $\chi_{eq} \approx 50^\circ$.

We will also use the torque proposed by Philippov et al. (2014):

$$\boldsymbol{K}_{PTL} = \frac{m^2\Omega^3}{c^3}\left(\boldsymbol{\varepsilon}_m k_2 \cos\chi - \boldsymbol{e}_z\left(k_0 + k_1\sin^2\chi + k_2\cos^2\chi\right)\right.$$
$$\left. + \zeta\frac{c}{\Omega r_{ns}}[\boldsymbol{e}_z \times \boldsymbol{\varepsilon}_m]\cos\chi\right), \tag{142}$$

where the values of the coefficients are obtained by the fitting of the results of MHD simulations of pulsar magnetosphere: $k_0 = 1$, $k_1 = 1.2$, $k_2 = 1$, $\zeta \approx 0.1$ (Philippov et al. 2014; Philippov, private communication). This torque makes all pulsars evolve to the orthogonal state. Corresponding inclination angle trajectories are given in Fig. 5.

6 INCLINATION ANGLE EVOLUTION

The presence of liquid core changes the situation dramatically. The initial flow having relaxed to quasi-stationary state, the long-term rotation dynamics can be described by equations (66)–(68). We also have to wait until the magnetic field will be expulsed from the core to use the coefficients S_2 and S_3 obtained in this paper.

The viscosity essentially depends on temperature. Therefore, in order to close the system of equations the star thermal evolution should be taken into consideration. The latter practically does not depend on spin evolution. It is determined mostly by star mass. It means that the viscosity can be considered as a known function of star age.

Coefficient S_3 describing the influence of anomalous torque on the inclination angle evolution grows with viscosity during the star cooling. It also depends on star angular velocity which decreases during the star braking. Moreover,

$$\tilde{k}_\perp = \zeta\frac{c}{\Omega r_{ns}}\cos\chi \tag{143}$$

depends on Ω and grows during star braking as well. Thus, the influence of anomalous torque on the inclination angle evolution increases with neutron star age.

In order to incorporate the thermal evolution into the model, we used the cooling code developed by Gnedin et al. (2001). We took a light neutron star with mass $\approx 1\,M_\odot$ with APR I equation of state (Heiselberg & Hjorth-Jensen 1999; Gusakov et al. 2005) and core neutron and proton superfluidity models given in Fig. 6 (Gusakov et al. 2005).

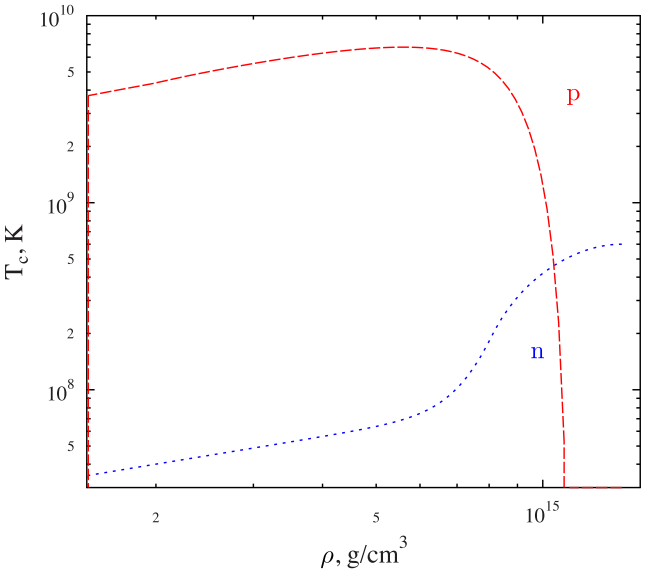

Figure 6. Critical temperatures for core protons (p) and neutrons (n) as functions of density ρ taken from Gusakov et al. (2005).

The neutron stars with small masses cool down more slowly than the heavy ones. Thus, a light star provides the lower bound for S_2 and S_3 at the given star age.

We calculated S_2 and S_3 using non-superfluid formulas (96) at all stages of evolution. To estimate the shear viscosity coefficient, we used formula (Gusakov, Chugunov & Kantor 2013)

$$\eta = 6\times10^{18}\left(\frac{\rho}{10^{15}\ \mathrm{g\,cm^{-3}}}\right)^2\left(\frac{T}{10^9\ \mathrm{K}}\right)^{-2}\left(\frac{T_{\rm cp}}{2\times10^9\ \mathrm{K}}\right)^{1/3}\times\frac{\mathrm{g}}{\mathrm{cm\ s}} \quad (144)$$

which is based on the results obtained by Shternin & Yakovlev (2008). Note that this formula is valid when $T < 0.2T_{\rm cp}$. We took $\rho^{(b)}$ to be equal to $1.5\times10^{14}\mathrm{g\,cm^{-3}}$. The used proton superfluidity model gives $T_{\rm cp}\approx 3\times10^9$ K for this density.

The calculated trajectories for different initial periods and inclination angles for pulsars with different relations $I_{\rm crust}/I_{\rm core}$ under the action of BPT and PTL torques are given in Figs 7–12.

7 DISCUSSION

One can see that the inclination angle trajectories in Figs 7–12 dramatically differ from rigid-star trajectories given in Figs 4 and 5. The time-scale of inclination angle evolution decreases by factor $\sim I_{\rm crust}/I_{\rm tot}$ and can be estimated as

$$\tau_{\rm ang.ev.}\sim\frac{I_{\rm crust}\Omega}{K_0}\approx1.3\times10^8\left(\frac{P}{1\ \mathrm{s}}\right)^2\frac{I_{\rm crust45}}{B_{012}^2}\ \mathrm{yr}, \quad (145)$$

while the braking time-scale does not change:

$$\tau_{\rm braking}\sim\frac{I_{\rm tot}\Omega}{K_0}\approx1.3\times10^8\left(\frac{P}{1\ \mathrm{s}}\right)^2\frac{I_{\rm tot45}}{B_{012}^2}\ \mathrm{yr}. \quad (146)$$

Here, $I_{\rm tot45}$ and $I_{\rm crust45}$ are the total and crust moments of inertia in the unities of $10^{45}\mathrm{gcm^2}$. It results in that the trajectories become much steeper in the $P-\cos\chi$ plane.

The pulsars tend to their equilibrium angles ($\chi_{\rm eq}\approx50^\circ$ in Figs 7 and 8, $\chi_{\rm eq}=90^\circ$ in Figs 9 and 10, $\chi_{\rm eq}=0^\circ$ in Figs 11 and 12). However, anomalous torque forces all pulsars to evolve to the orthogonal state. The young neutron stars are hot, Ekman number is very small and anomalous torque practically does not participate in the inclination angle evolution. When the age of neutron star reaches few millions years (or even earlier for more heavier stars) the temperature of the core drops by several orders of magnitude, S_3 becomes large enough and, as one can see, all trajectories sharply turn upwards at these time-scales.

The pulsars which are born fast rotating slow down up to a few hundreds of milliseconds until they become orthogonal. However, if a pulsar was born with initial period >100 ms, it becomes orthogonal rotating before its period changes significantly. The evolution trajectories of such pulsars look almost like vertical lines in the $P-\cos\chi$ plane. It means that the observed period distribution should almost coincide with initial period distribution in the area of large periods. However, the initial period distributions constructed by different independent methods have a maximum $\approx0.1-0.3$ s. Pulsars practically are not born with periods >1 s (Popov & Turolla 2012; Igoshev & Popov 2013; Noutsos et al. 2013). Moreover, we should observe a large amount of old pulsars with inclination angles close to 90°. The real inclination angle distribution is more dense in the small angles area. Thus, the obtained trajectories seems to contradict the observations.

The first and most obvious explanation of this contradiction is that the basic assumption of this paper is incorrect. Viscosity cannot be the main crust–core interaction mechanism. An important role should play the magnetic field penetrating the core. In this case, charged component is coupled with crust at much shorter time-scale (Easson 1979) and acceleration effect is proportional rather to $I_{\rm tot}/(I_{\rm tot}-I_{\rm sf})$ than $I_{\rm tot}/I_{\rm crust}$ (Barsukov et al. 2013b), where $I_{\rm sf}$ is the moment of inertia of superfluid neutrons which can be quite small for some superfluid models. Coefficients S_2 and S_3 are determined by mutual friction.

There are some possibilities to make the model more appropriate. First, some authors have obtained the electromagnetic torques without anomalous term (Michel 1991; Istomin 2005). In this case, the inclination angle evolution accelerates by factor $I_{\rm tot}/I_{\rm crust}$ as before. However, if electromagnetic torque allows the existence of equilibrium inclination angle (like BPT-torque), the model remains consistent with observational data.

Another assumption that has been made is that the shape of neutron star is perfectly spherical. In reality, it is not so. First of all, the star is deformed by rotation. To take this into account, one just needs to replace $I_{\rm crust}$ by $I_{\rm crust}+\Delta I$, where ΔI is the small correction to the crust moment of inertia caused by the deformation. This kind of deformation practically does not change anything.

The neutron star also should be deformed by own magnetic field. It can be shown (Barsukov & Tsygan 2010) that this kind of deformation can be taken into account with replacing ζ by

$$\zeta_{\rm eff}=\zeta-12l\frac{r_{\rm ns}}{r_{\rm g}}\frac{I_{\rm crust}}{M_{\rm ns}r_{\rm ns}}, \quad (147)$$

where $r_{\rm g}$ is the neutron star gravitation radius, l is the coefficient determined through the relation (Haskell et al. 2008)

$$\frac{\Delta I}{I_{\rm crust}}=l\frac{B_0^2r_{\rm ns}^4}{GM_{\rm ns}}. \quad (148)$$

The value of this coefficient substantially depends on the EOS and internal magnetic field configuration. If it is large enough, $\zeta_{\rm eff}$ becomes negative and at the final stage all pulsars will evolve to coaxial state instead orthogonal. One can imagine the following scenario. Young pulsar evolves to orthogonal state under the action of external torque and locates in this state until it cools down enough. After that the pulsar rapidly falls down (in $\cos\chi-$age plane) into coaxial state where it ends its life as a radio pulsar. Therefore, the observed pulsars with large periods should be on 'retrograde motion' stage. The required wide dispersion of the 'retrograde motion' periods can be related with dispersion of $\zeta_{\rm eff}$ and other possible neutron star parameters.

Finally, crystalline crust, in principle, can maintain an arbitrarily oriented deformation which causes an additional precession and for rigid star can prevent the pulsar alignment (Goldreich 1970). However, the origin of such the deformations is not clear. Moreover, it seems to be not very plausible that this kind of deformations can survive on long-term evolution time-scale. In any case, together with magnetic deformation it makes a neutron star triaxial. The rotation of such stars requires a separate study.

Recently, Lyne et al. (2013) argued that the observed changes in radio emission profile of Crab pulsar can be interpreted as a direct observation of the inclination angle evolution. They found that the separation between main pulse and interpulse increases with time-scale $\sim10^4$ yr. It is pretty slow evolution for the pulsar with $P=0.033$ ms and $B_{012}=7.56$ (Manchester et al. 2005), especially in the framework of proposed model. However, this result can be made consistent with the model if we suppose that the Crab pulsar evolve under the action of BPT-torque. A pulsar with $P_0\approx10$ ms a several hundred years after birth should reach its torque equilibrium

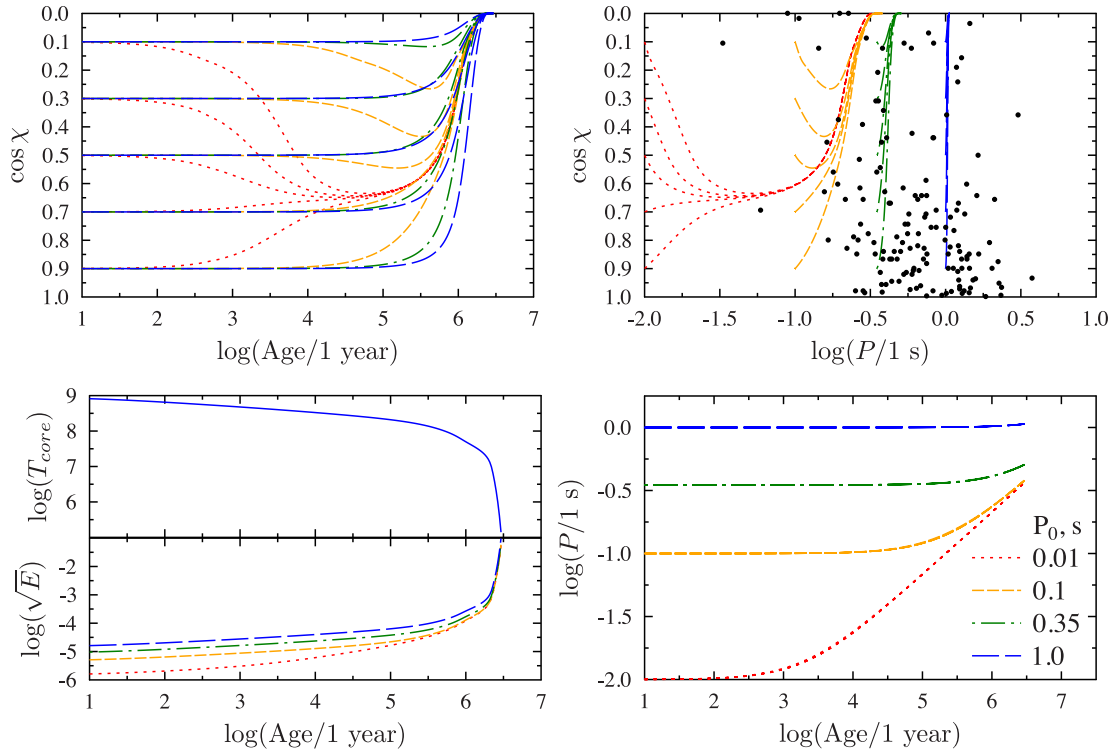

Figure 7. The evolution trajectories for pulsars with different initial periods and inclination angles in the $\cos\chi-$age (top-left panel), $P-$age (bottom-right panel) and $\cos\chi-P$ (top-right panel) planes. Observational data shown by dots are taken from Rankin (1993). Relation $I_{\rm crust}/I_{\rm core}$ is put to be equal to 0.1. Pulsars evolves under the action of BPT-torque. The magnetic field strength at the poles is taken to be equal to 10^{12} G, $\nu_{\rm nd}=0.5$. The bottom-left panel shows the evolution of core temperature and $\sqrt{E}$.

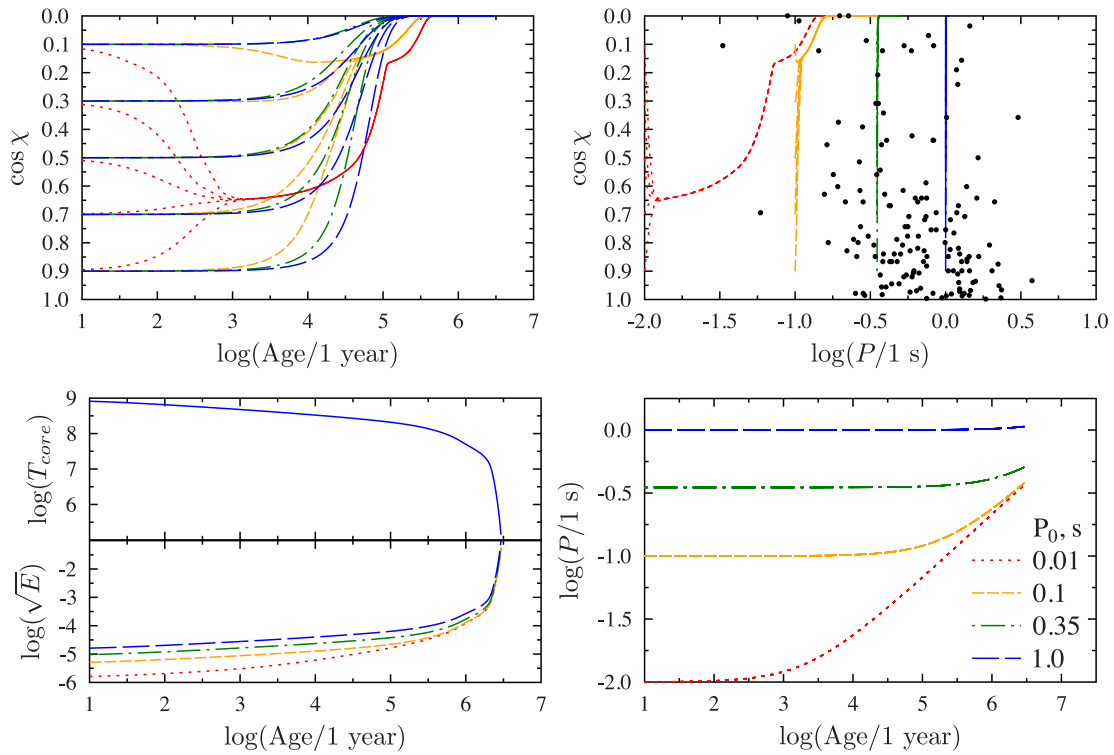

Figure 8. The same as in Fig. 7 for $I_{\rm crust}/I_{\rm core}=0.01$. The knee near $\cos\chi=0.15$ is related with the features of $\bar{\alpha}$ model (see Barsukov et al. 2013a for the detail).

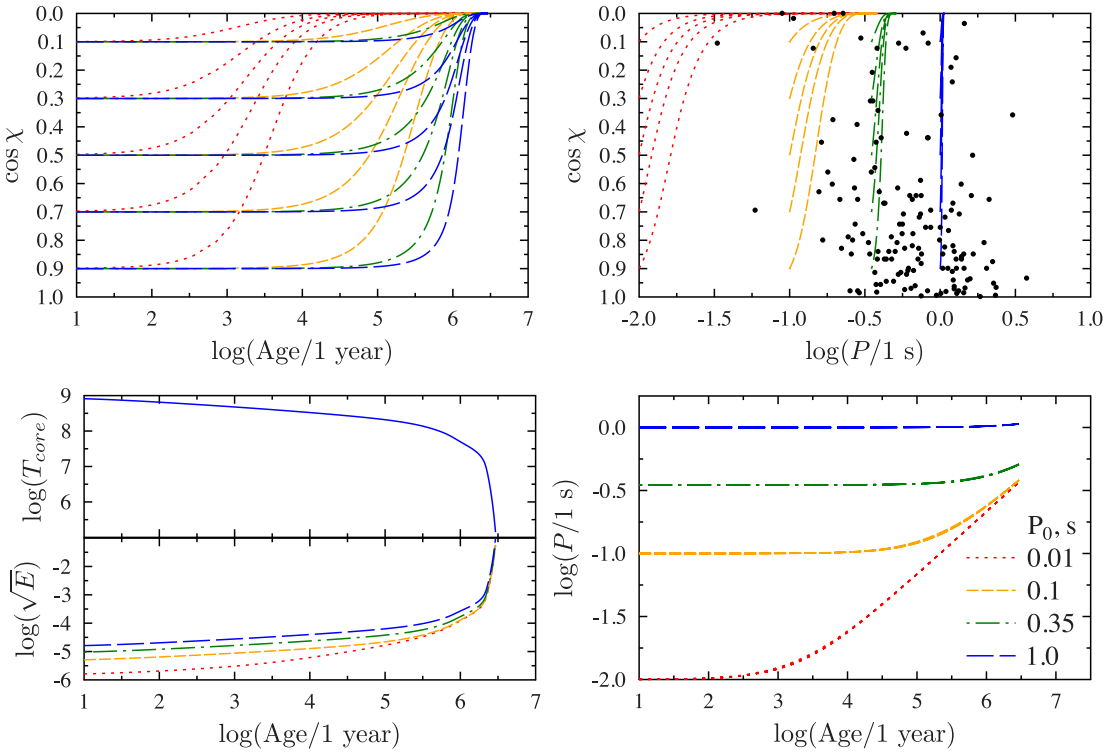

Figure 9. The same as in Fig. 7 for $\nu_{\rm nd} = 0$.

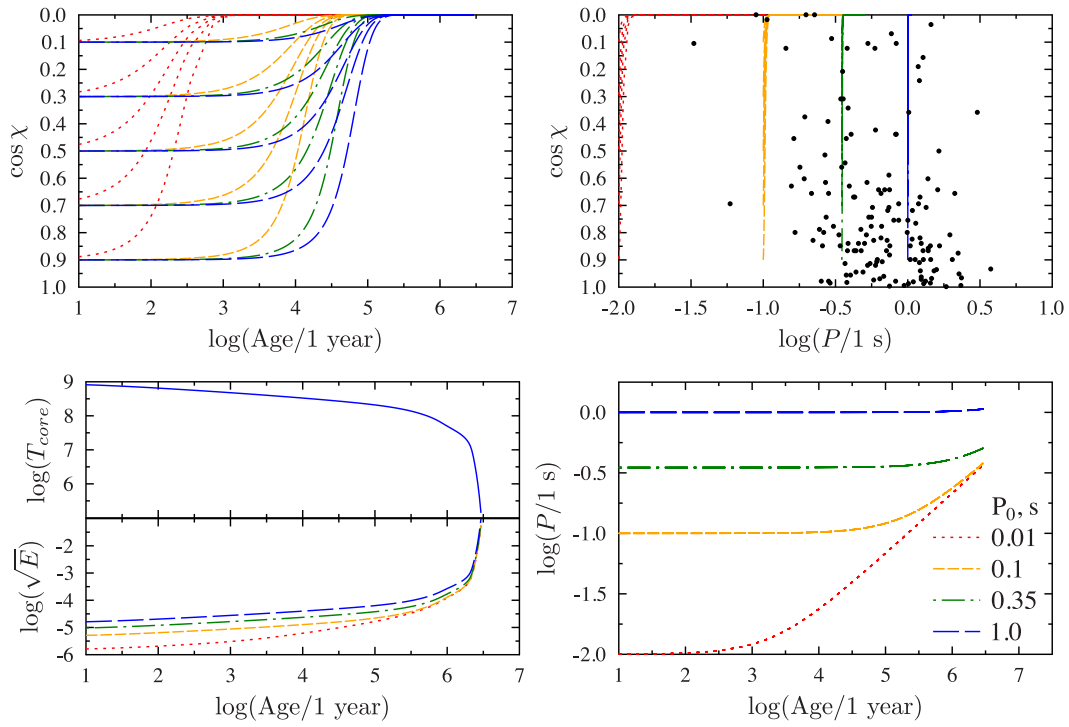

Figure 10. The same as in Fig. 7 for $\nu_{\rm nd} = 0$ and $I_{\rm crust}/I_{\rm core} = 0.01$.

angle (see Fig. 8). After it happens the further inclination angle evolution is determined by changing of Ω, S_2 and S_3 with time. This evolution is quite slow for young pulsars. If it is so for Crab pulsar, its observable inclination angle lying between 45° and 70° (see the references in Lyne et al. 2013) requires the non-dipolarity parameter $\nu_{\rm nd} = 0.2-0.6$.

Our model does not take into account any glitch phenomena. These processes are fundamentally not quasi-stationary and there is not one point of view what physical processes are responsible for these phenomena. The glitches probably can be included into the model in some phenomenological way.

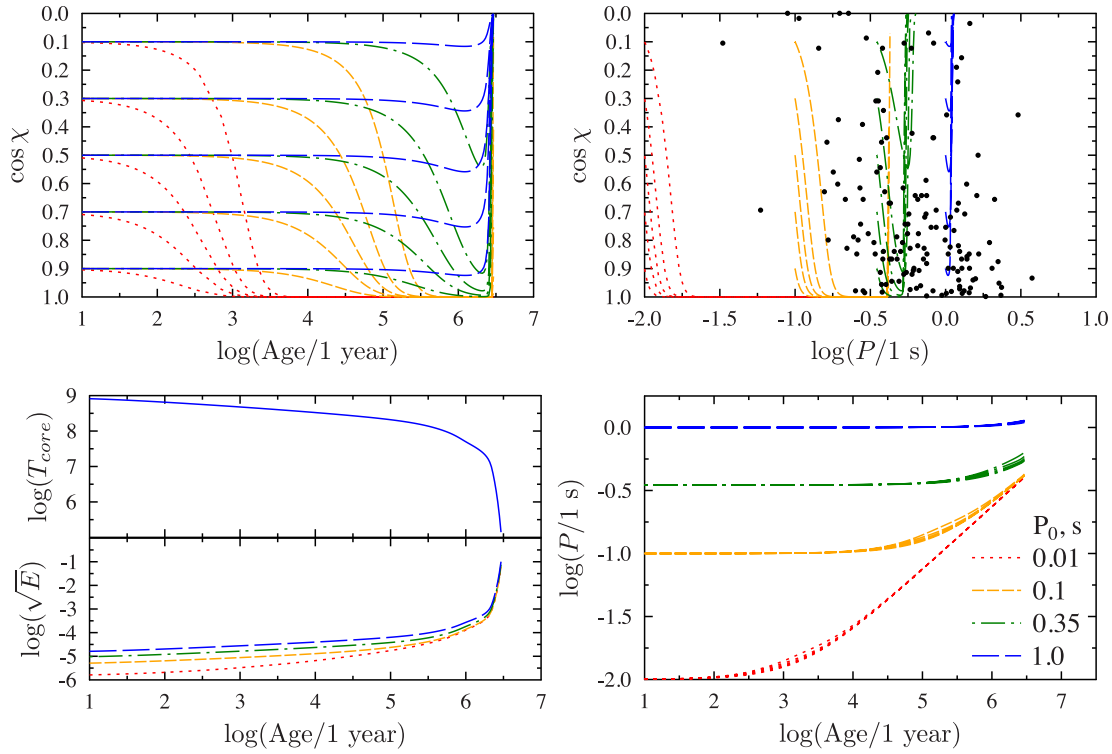

Figure 11. The same as in Fig. 7 for PTL-torque.

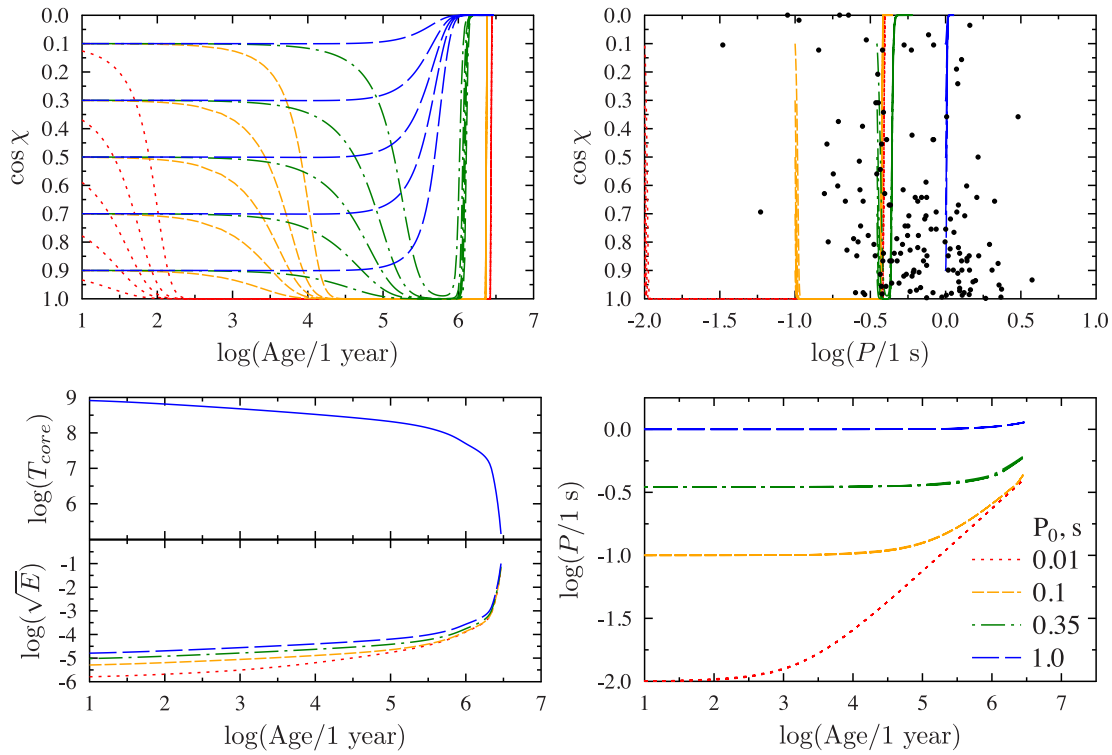

Figure 12. The same as in Fig. 11 for $I_{\rm crust}/I_{\rm core} = 0.01$.

ACKNOWLEDGEMENTS

The authors are grateful to M. E. Gusakov, A. A. Philippov and D. A. Shalybkov for helpful discussions. The authors also would like to thank the referee for the useful comments. This work was partly supported by the Russian Foundation for the Basic Research (project 13-02-00112), the Programme of the State Support for Leading Scientific Schools of the Russian Federation (grant NSh-4035.2012.2) and Ministry of Education and Science of Russian Federation (Agreement No. 8409).

REFERENCES

Abney M., Epstein R. I., 1996, J. Fluid Mech., 312, 327
Barsukov D. P., Tsygan A. I., 2010, MNRAS, 409, 1077
Barsukov D. P., Polyakova P. I., Tsygan A. I., 2009, Astron. Rep., 53, 1146
Barsukov D. P., Goglichidze O. A., Tsygan A. I., 2013a, Astron. Rep., 57, 26
Barsukov D. P., Goglichidze O. A., Tsygan A. I., 2013b, MNRAS, 432, 520
Baym G., Chandler E., 1983, J. Low Temp. Phys., 50, 57
Beskin V., 2009, Astronomy and astrophysics library, MHD Flows in Compact Astrophysical Objects: Accretion, Winds and Jets. Springer-Verlag, Berlin
Beskin V. S., Gurevich A. V., Istomin I. N., 1983, Sov. J. Exp. Theor. Phys., 58, 235
Beskin V. S., Istomin Y. N., Philippov A. A., 2013, Phys.-Usp., 56, 164
Buckley K. B., Metlitski M. A., Zhitnitsky A. R., 2004, Phys. Rev. Lett., 92, 151102
Casini H., Montemayor R., 1998, ApJ, 503, 374
Davis L., Goldstein M., 1970, ApJ, 159, L81
Easson I., 1979, ApJ, 233, 711
Gnedin O. Y., Yakovlev D. G., Potekhin A. Y., 2001, MNRAS, 324, 725
Goldreich P., 1970, ApJ, 160, L11
Gourgouliatos K. N., Cumming A., Reisenegger A., Armaza C., Lyutikov M., Valdivia J. A., 2013, MNRAS, 434, 2480
Greenspan H., 1990, Cambridge Monographs on Mechanics and Applied Mathematics, The Theory of Rotating Fluids. Cambridge Univ. Press, Cambridge
Gusakov M. E., Kaminker A. D., Yakovlev D. G., Gnedin O. Y., 2005, MNRAS, 363, 555
Gusakov M. E., Chugunov A. I., Kantor E. M., 2013, preprint (arXiv:1305.3825)
Haensel P., Levenfish K. P., Yakovlev D. G., 2000, A&A, 357, 1157
Haensel P., Levenfish K. P., Yakovlev D. G., 2001, A&A, 372, 130
Hall H. E., Vinen W. F., 1956, Proc. R. Soc. A, 238, 215
Haskell B., Samuelsson L., Glampedakis K., Andersson N., 2008, MNRAS, 385, 531
Heiselberg H., Hjorth-Jensen M., 1999, ApJ, 525, L45
Igoshev A. P., Popov S. B., 2013, MNRAS, 432, 967
Istomin Y. N., 2005, in Wass A. P., ed., Progress in Neutron Star Research Magnetodipole Oven. Nova Science Publishers, New York, p. 27
Jones P. B., 1976, ApJ, 209, 602
Khalatnikov I., 2000, Advanced Book Classics, An Introduction To The Theory Of Superfluidity. Westview Press, Boulder, CO
Landau L. D., Lifshitz E. M., Sykes J. B., Reid W. H., 1959, Fluid Mechanics. Pergamon Press, Oxford
Link B., 2006, A&A, 458, 881
Lyne A., Graham-Smith F., Weltevrede P., Jordan C., Stappers B., Bassa C., Kramer M., 2013, Science, 342, 598
Manchester R. N., Hobbs G. B., Teoh A., Hobbs M., 2005, AJ, 129, 1993
Melatos A., 2000, MNRAS, 313, 217
Mendell G., 1991, ApJ, 380, 515
Michel F. C., 1991, Theory of Neutron Star Magnetospheres. Univ. Chicago Press, Chicago, IL
Noutsos A., Schnitzeler D. H. F. M., Keane E. F., Kramer M., Johnston S., 2013, MNRAS, 430, 2281
Philippov A., Tchekhovskoy A., Li J. G., 2014, MNRAS, 441, 1879
Pons J. A., Miralles J. A., Geppert U., 2009, A&A, 496, 207
Popov S. B., Turolla R., 2012, Ap&SS, 341, 457
Rankin J. M., 1993, ApJS, 85, 145
Reisenegger A., 1995, ApJ, 442, 749
Shternin P. S., Yakovlev D. G., 2008, Phys. Rev. D, 78, 063006
Spitkovsky A., 2008, in Bassa C., Wang Z., Cumming A., Kaspi V. M., eds, AIP Conf. Proc., Vol. 983 40 Years of Pulsars: Millisecond Pulsars, Magnetars and More. Am. Inst. Phys., New York, p. 20
Tilley D., Tilley J., 1990, Graduate Student Series in Physics, Superfluidity and Superconductivity. Hilger, Bristol
van Eysden C. A., Melatos A., 2013, J. Fluid Mech., 729, 180
Yakovlev D. G., Levenfish K. P., Shibanov Y. A., 1999, Phys.-Usp., 42, 737

This paper has been typeset from a TEX/LATEX file prepared by the author.